The Role of α-ENaC and δ-ENaC in Breast Cancer Cell Migration

Hiroki Ambalawanar

Supervisor: Associate Professor Fiona McDonald

Thesis submitted in partial fulfilment for the degree of

Bachelor of Biomedical Science with Honours

School of Biomedical Sciences, Department of Physiology

University of Otago, Dunedin

October 2019

Abstract

Breast cancer is an important disease worldwide, primarily affecting women, and is the most common and deadliest form of female cancer. This is reflected in New Zealand's population as breast cancer has high incidence and mortality rates. In New Zealand, almost 700 deaths occur each year due to breast cancer, with a majority due to metastases.

The progression of cancer into a metastatic disease requires a change in cell phenotype, possibly through a process called epithelial-to-mesenchymal transition (EMT). When EMT occurs, fully epithelial cells, with cell to cell junctions and apical-basolateral polarity, transition into cells with a mesenchymal phenotype, becoming more invasive and motile and changing their morphology. Ion channels are reported to be important regulators of EMT including some evidence for a role of the epithelial sodium channel (ENaC). ENaC mRNA expression has been correlated with prognosis in breast cancer patients. Aldosterone, which increases ENaC mRNA and protein in other tissue, has been shown to alter breast cancer cell migration. This suggests that ENaC may have a role in breast cancer cell migration.

The aims of this project were to understand the role of α-ENaC and δ-ENaC in breast cancer cell migration by increasing and decreasing their expression within the cells. My hypotheses were "overexpression of α-ENaC or δ-ENaC will cause an increase in breast cancer cell migration" and "knockdown of α-ENaC or δ-ENaC will cause a decrease in breast cancer cell migration".

Two breast cancer cell lines, BT-549 and MDA-MB-231, were used in this project to model breast cancer cell migration. These cells were transfected to either overexpress or knockdown α-ENaC or δ-ENaC. Scratch assays were then performed to quantify any changes in migration speed of the cells. The cells were then lysed and underwent qPCR to validate the overexpression or

knockdown. To compare the role of ENaC in breast cancer cell migration, a two-way ANOVA was performed.

Overexpression or knockdown of α-ENaC in MDA-MB-231 and BT-549 cells did not significantly alter migration of the cells compared to control cells. Results from qPCR analysis showed successful overexpression of α-ENaC. Similarly, overexpression or knockdown of δ-ENaC in MDA-MB-231 and BT-549 cells did not significantly alter migration of the cells. Results from the qPCR showed overexpression of δ-ENaC in both cell lines was successful. Results from qPCR experiments have shown that attempts to knockdown of α-ENaC and δ-ENaC were unsuccessful in both cell lines.

The results did not support the hypothesis that altering levels of α-ENaC or δ-ENaC would change the rate of breast cancer cell migration, although a second migration assay should be used to confirm these results. Therefore, ENaC may be regulating another pathway, such as proliferation, to contribute to EMT.

Acknowledgements

Firstly, I would like to express my gratitude to my supervisor Associate Professor Fiona McDonald. Thank you for your guidance, encouragement, and time throughout the year.

I would also like to thank those that helped with the completion of my project this year. To Dr Adam Ware, thank you for the introductory practical training and providing me with helpful suggestions. To Sarah McQueen, thank you for showing me how to perform and analyse scratch assay experiments and thank you to you both for taking the time to proof-read my work throughout the year. To Sahib Rasulov, thank you for your help with conducting qPCR and answering any lab related questions I have had throughout the year. To all the other members of the McDonald/Hamilton laboratories, thank you for the support and helpful suggestions.

Finally, to my family and friends, thank you for the words of support and encouragement throughout the year.

Table of Contents

List of Figures

List of Tables

List of Abbreviations

A = Ampere

ANOVA = Analysis of Variance

ASIC1 = Acid-Sensing Ion Channel 1

BLAST = Basic Local Alignment Search Tool

BMI = Body Mass Index

bp = Base Pairs

BRCA1/2 = Breast Cancer Susceptibility Gene Type 1 and 2

BSA = BreastScreen Aotearoa

c = Concentration

cDNA = Complementary Deoxyribonucleic Acid

CFTR = Cystic Fibrosis Transmembrane Conductance Regulator

cm = Centimetre

CO_2 = Carbon Dioxide

DCIS = Ductal Carcinoma in Situ

DNA = Deoxyribonucleic Acid

EGFR = Epidermal Growth Factor Receptor

EMT = Epithelial to Mesenchymal Transition

ENaC = Epithelial Sodium Channel

ERK = Extracellular Signal-Regulated Kinases

FBS = Foetal Bovine Serum

g = Gram

GAPDH = Glyceraldehyde 3-phosphate Dehydrogenase

GPER = G Protein Estrogen Receptor

HER-2 = Human Epidermal Growth Factor Receptor 2

hERG1= Human Ether-à-go-go-Related Gene 1

L = Litre

mCCD = Mouse Cortical Collecting Duct

MET = Mesenchymal to Epithelial Transition

min = Minute(s)

mL = Millilitre

mm = Millimetre

mM = Millimolar

MR = Mineralocorticoid Receptors

mRNA = Messenger Ribonucleic Acid

N = Number of Biological Repeats

n = Number of Experimental Repeats

NHE1 = Sodium-Hydrogen Antiporter 1

nM = Nanomolar

PBS = Phosphate-Buffered Saline

PHA1 = Pseudohypoaldosteronism Type 1

pmol = Picomole

pM = Picomolar

Prrx1 = Paired Related Homeobox 1

qPCR = Quantitative Polymerase Chain Reaction

RPM = Revolutions Per Minute

RAAS = Renin Angiotensin Aldosterone System

RT-PCR = Reverse Transcription Polymerase Chain Reaction

RVI = Regulatory Volume Increase

SEM = Standard Error of the Mean

SERPINA3 = Serpin Peptidase Inhibitor, clade A Member 3

shRNA = Short Hairpin Ribonucleic Acid

siRNA = Small Interfering Ribonucleic Acid

SGK1 = Serum and Glucocorticoid-Regulated Kinase 1

TMN = Tumour Node Metastasis

TRMP7 = Transient Receptor Potential-Melastatin-Like 7

V = Voltage

v = Volume

VSMC = Vascular Smooth Muscle Cell

W = Watt

α = Alpha

β = Beta

δ = Delta

γ = Gamma

µL = Microlitre

µg = Microgram

˚C = Degrees Celsius

% = Percent

~ = Approximately

± = Plus/Minus

1 Introduction

1.1 Breast Cancer

1.1.1 Epidemiology

Breast cancer in an important disease worldwide with it being the most common and deadliest form of cancer in females (Bray *et al.*, 2018). GloboCan 2018, produced by the International Agency for Research on Cancer, estimated that almost a quarter of new female cancer and 15% of female cancer deaths were due to breast cancer. They also found that the Australia/New Zealand region had the highest age-standardised rate of breast cancer at 94.2 cases per 100,000 females (Bray *et al.*, 2018). This is supported by figures from the Ministry of Health that show a high burden in New Zealand population, especially on the Māori population. In 2017, an age standardised incidence rate of 130 cases per 100,000 females was reported for Māori and 90 cases per 100,000 females for non-Māori (Ministry of Health, 2019). This trend is also seen in mortality data from 2016 with an age standardised mortality rate of 21.8 deaths per 100,000 females for Māori compared to 16.8 deaths per 100,000 females for non-Māori (Ministry of Health, 2018). Approximately 700 women in New Zealand die each year due to breast cancer, with the majority of breast cancer deaths due to metastases (Jin & Mu, 2015; Ministry of Health, 2018).

1.1.2 Classification

Breast cancer is a heterogeneous disease and can be classified in different ways. These include histological grade and subtype, stage of disease, and molecular subtype. These different classifications can predict the prognosis of the patients with different treatment strategies employed for different classifications.

Breast cancer can be classified based on the appearance of biopsied cells into a histological subtype and grade. Histological subtype refers to classification of breast cancer cells based upon the different morphological and cytological features of the cell and how they may impact the disease (Weigelt *et al.*, 2010). The World Health Organisation reports many different subtypes with most common being "Invasive breast carcinoma, no special type" which accounts for approximately 55% of all breast cancer (Makki, 2015). This subtype includes all breast carcinoma that do not have enough features to justify classification of a special type. Special types of breast carcinoma make up 25% of all breast cancer with common subtypes including invasive lobular carcinoma, medullary carcinoma, and invasive cribriform carcinoma (Weigelt *et al.*, 2010; Sinn & Kreipe, 2013). Another important histologically identified subtype is ductal carcinoma in situ (DCIS). DCIS is a pre-cancerous growth that can develop into invasive carcinomas (Sinn & Kreipe, 2013; Makki, 2015). The histological grade of breast cancer can also be determined based on appearance. This is based on tubule formation, nuclear pleomorphism, and mitotic count (Elston & Ellis, 1991). Breast cancer grade can be classified as I, for well differentiated, II, for moderately differentiated, and III, for poorly differentiated with grade III having the worst prognosis (Elston & Ellis, 1991).

Breast cancer can also be classified based on the stage of disease. Tumour Node Metastasis (TNM) staging is based on three factors: size of the primary tumour (T), number of regional lymph nodes affected (N), and whether metastases has occurred (M) (Giuliano *et al.*, 2017). There are four stages I, II, III, and IV with stage IV having the worst prognosis. Tumour size ranges from T0, with no evidence of a primary tumour, to T4, where the tumour causes a direct extension of the chest wall or skin. The number of regional axillary lymph nodes affected

determines the classification of N0 to N3, with the classification escalating as the number of affected lymph nodes increases. This denotes the cells from the primary tumour that are able to migrate into the axillary lymph nodes. If the cells are able to travel further and seed in different organs, this is referred to as metastases, leading to a classification of M1 rather than M0 for no metastases. Different combinations of these lead to staging with metastases being a requirement for a stage IV classification (Giuliano *et al.*, 2017).

The molecular subtypes of breast cancer are based on the expression of different markers that affect prognosis. The markers include oestrogen and progesterone hormone receptor status, human epidermal growth factor receptor 2 (HER-2) status, and the level of Ki67 proliferation marker. There are five molecular subtypes which include Luminal A, Luminal B HER-2 negative, Luminal B HER-2 positive, HER-2 positive, and Basal-like or Triple Negative (**Table 1.1**) (Goldhirsch *et al.*, 2011). Each of these have different prognoses and treatment strategies based on the expression of the molecular targets. Luminal A breast cancer has the highest 5-year all cause survival at 91.9% and triple negative has the lowest at 76.7% (Lawrenson *et al.*, 2018).

Table 1.1: Breast Cancer subtype characteristics, prevalence, and 5-year all causes survival (1: Goldhirsch et al., 2011; 2: Lawrenson et al., 2018)

Subtype [1]	Characteristics [1]	Prevalence [2]	5-year Survival [2]
Luminal A	Oestrogen and/or Progesterone Positive HER-2 Negative Low Ki-67 (<14%)	62.2%	91.9%
Luminal B HER-2 Negative	Oestrogen and/or Progesterone Positive HER-2 Negative High Ki-67	12.2%	81.6%
Luminal B HER-2 Positive	Oestrogen and/or Progesterone Positive HER-2 Positive Any Ki-67	8.8%	87.5%
HER-2 Positive	Oestrogen and/or Progesterone Negative HER-2 Positive	5.8%	78.1%
Basal-like (Triple Negative Breast Cancer)	Oestrogen and/or Progesterone Negative HER-2 Negative	11.0%	76.7%

1.1.3 Risk Factors and Treatments

Interventions to reduce the occurrence of breast cancer require an understanding of the risk factors associated with the development of breast cancer. These risk factors include age, lifestyle factors, reproductive factors, and genetics. Age is an important risk factor in the development of breast cancer as older women are at a higher risk of developing breast cancer. In New Zealand, a majority of new breast cancer diagnoses in 2016 occurred in women over the age of 45 (Ministry of Health, 2019). Lifestyle factors such as low physical activity, high body mass index (BMI), poor diet, and high alcohol consumption all increase the risk of developing breast cancer (Rojas & Stuckey, 2016). The reproductive factors of a women are also important predictors of breast cancer development. Early age of menarche, older age at

first child birth, low parity, and later age of menopause all contribute to increased risk of developing breast cancer (Horn *et al.*, 2013). Genetics can also influence the risk of developing breast cancer, with breast cancer susceptibility gene type 1 and 2 (BRCA1/2) as a well-known example. BRCA1 is located on chromosome 17q21, and BRCA2 is located on chromosome 13q12. These are anti-tumour genes and so mutations lead to an increased risk of breast cancer (Sun *et al.*, 2017). The cumulative risk of developing breast cancer by age 70 was 57% for BRCA1 carriers and 49% for BRCA2 carriers (Chen & Parmigiani, 2007).

While some of these risk factors can be modified to lower risk of developing breast cancer, others cannot so these women may be at higher risk of developing breast cancer and should be closely monitored. This could be accomplished through breast cancer screening initiatives such as BreastScreen Aotearoa (BSA). BSA is a breast cancer screening programme in New Zealand that offers a free mammogram every two years to women aged 45 to 69 years. This enables early detection of breast cancer, leading to a better prognosis. Screen detected cancers were more likely to be small, localised, low grade, and less advanced tumours when to non-screen detected tumours (Ministry of Health, 2015; Seneviratne *et al.*, 2016). An evaluation of BSA revealed that it was responsible for a 34% decrease in mortality between screened and non-screened women, between the years of 1999 to 2011 (Ministry of Health, 2015). Increasing accessibility to screening will allow for increased detection of early stage breast cancers to which effective treatments are available. Screen detection of advanced and metastatic breast cancers would likely have little effect on prognosis due to ineffective treatments. Therefore, more research is required to develop efficacious therapies to reduce deaths caused by advanced breast cancers.

The current treatments for breast cancer vary with breast cancer subtype. Surgery to remove the primary tumour is usually the first step in breast cancer treatment either by mastectomy, where all the breast tissue is removed, or more commonly breast conserving surgery, where only the affected regions are removed (Matsen & Neumayer, 2013). Axillary lymph nodes may be removed based on whether the sentinel node or the first axillary lymph node, contain cancer cells. If the sentinel node is clear of cancer cells, no more axillary lymph nodes are required to be removed (Matsen & Neumayer, 2013; Davies, 2016). Other treatments include Radiation therapy, Chemotherapy, Hormone therapy, and other targeted treatments including trastuzumab. Radiation therapy is a targeted therapy that involves administering beams of radiation to affected regions after surgery to kill any remaining tumour cells (Breast Cancer Foundation NZ, 2019). Another treatment option is chemotherapy which is a systemic treatment. Chemotherapy targets fast proliferating cells such as cancer cells and can be administered before surgery to reduce the size of the primary tumour, or after surgery to kill any remaining tumour cells that may have escaped surgical removal (Breast Cancer Foundation NZ, 2019). Anthracyclines and Taxanes are the standard chemotherapy treatments, administered over a four to six month period (Davies, 2016; Breast Cancer Foundation NZ, 2019). Hormone therapy is another therapeutic option that can be used against breast cancer subtypes expressing the oestrogen or progesterone hormone receptors. These subtypes receive growth signals from oestrogen and progesterone circulating in the body. Hormone therapy works by blocking these signals and slowing tumour growth. Tamoxifen and aromatase inhibitors are examples of hormone therapies (Davies, 2016; Breast Cancer Foundation NZ, 2019). Breast cancer subtypes expressing the HER-2 receptor can be treated

with trastuzumab, an anti-HER-2 monoclonal antibody. This binds to the receptor, stopping it from binding its targets and receiving growth signals (Harbeck & Gnant, 2017; Breast Cancer Foundation NZ, 2019).

1.1.4 Metastasis

Metastases occur when cells from the primary tumour are able to escape and seed within distant organs. With metastatic breast cancer, this usually occurs within the brain, bones, and lungs (Jin & Mu, 2015). Metastatic breast cancer is currently considered an incurable disease consequently resulting in a majority of breast cancer deaths. Current treatments are not very effective as metastatic breast cancer has a 5-year survival rate of only 26% (Li & Kang, 2016). Systemic treatments including chemotherapy, hormone therapy, and anti-HER-2 trastuzumab are currently being used depending on whether the subtype of the tumour expresses the targets. There are currently few effective treatments targeting metastases directly, therefore further research into pathways involved in cancer progression, such as how primary breast cancer cells acquire the ability to migrate to other areas of the body, is required. This progression may occur through a process called epithelial to mesenchymal transition (EMT).

1.2 Epithelial to Mesenchymal Transition (EMT)

1.2.1 EMT Process, Markers, Regulators

Epithelial to Mesenchymal Transition (EMT) is a process where fully differentiated epithelial cells transition into cells with a more mesenchymal phenotype. Epithelial cells lose cell-to-cell junctions and apical-basolateral polarity and gain mesenchymal characteristics including becoming more invasive and motile with a spindle-like morphology (**Figure 1.1**) (Zhang & Weinberg, 2018). EMT is a reversible process, with a spectrum of intermediate phenotypes available depending on the EMT transcription factors expressed as well as the tissue

environment (Zhang & Weinberg, 2018; Pastushenko & Blanpain, 2019). It was initially described as a developmental process and is now relevant in the context of cancer (Campbell, 2018).

EMT is a complex process with many intermediate transition states possible. This allows for speculation concerning the different roles these transition states may play in cancer progression. This means it could be possible for one transition state to be responsible for migration, another for invasion, another for proliferation and so on (Pastushenko & Blanpain, 2019). The state of transition that a cell is in is widely described based on the markers expressed by the cell. Markers of EMT include E-Cadherin as an epithelial marker and N-Cadherin and Vimentin as mesenchymal markers (Campbell, 2018). EMT transcription factors which include Snail, Slug, Twist, ZEB1, and ZEB2 can also be used as a marker to confirm whether EMT is occurring (Garg, 2013).

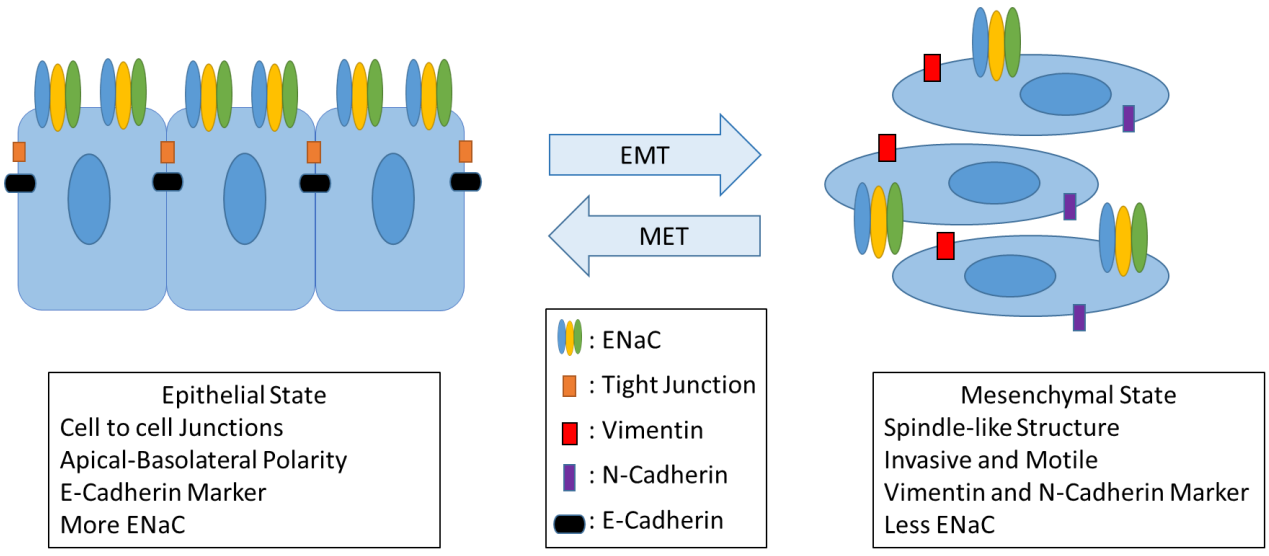

Figure 1.1 Original figure showing a phenotypic change with Epithelial to Mesenchymal Transition. The epithelial state has cell to cell junctions with apical-basolateral polarity. Epithelial state expresses E-Cadherin marker and higher ENaC mRNA. The mesenchymal state

has a spindle-like morphology with higher invasive and motile abilities. Mesenchymal state expresses Vimentin and N-Cadherin markers and lower ENaC mRNA.

1.2.2 Metastatic Cascade

For cancer to progress into metastases, the metastatic cascade must occur. This involves local invasion of surrounding tissue, intravasion into blood or lymphatic vessels, survival within the circulation, extravasion into a distant organ, survival in the new environment, and outgrowth within the new tissue (Valastyan & Weinberg, 2011; Jin & Mu, 2015). For these steps to occur, the cells must change phenotype and adopt characteristics that allow for this progression. Using EMT pathways, these cells can lose their cell to cell junctions and become more migratory and invasive (Jin & Mu, 2015). When arriving at the distant organ, the reverse process, Mesenchymal to Epithelial transition (MET), may occur to help seed the cell in the new environment (Wang & Zhou, 2011). The role of EMT in the progression of cancer is important and so understanding what regulates EMT, for instance ion channels, may help reduce the development of metastases.

1.2.3 Ion Channels and EMT

Ion channels have been shown to regulate EMT. Ion channels such as the human Ether-à-go-go-related gene 1 (hERG1), Cystic Fibrosis transmembrane conductance regulator (CFTR), and Transient receptor potential-melastatin-like 7 (TRMP7), have been shown to be involved in EMT (Zhang *et al.*, 2013; Davis *et al.*, 2014; Fortunato, 2017). A role of potassium channel, hERG1, in EMT was demonstrated by Fortunato (Fortunato, 2017). When hERG1 was silenced in mesenchymal HCT116 colorectal carcinoma cells, the morphology and proliferative ability was altered. The cells transitioned to become more flat with less membrane protrusions and became less proliferative. The expression of several EMT markers was quantified and showed that the hERG1 silenced cells had a more epithelial profile compared to the non-silenced cells

(Fortunato, 2017). The chloride and bicarbonate channel, CFTR, was also shown to be involved in EMT (Zhang *et al.*, 2013). When EMT was induced in MCF-7 epithelial breast cancer cells, a decrease in expression of CFTR and epithelial marker E-Cadherin was observed, with an increase in the cell's ability to migrate and invade. When CFTR was overexpressed in MDA-MB-231 mesenchymal breast cancer cells, , invasion and migration were repressed with an increase in the epithelial marker, E-Cadherin, and a decrease in the mesenchymal marker, Vimentin (Zhang *et al.*, 2013). Calcium channel, TRMP7, may also be involved in EMT (Davis *et al.*, 2014). TRMP7 plays an important role in mediating an intracellular calcium signal that was necessary for EMT to occur. When TRMP7 was knocked down, there was a reduction of the mesenchymal marker Vimentin that leads to a more epithelial phenotype (Davis *et al.*, 2014).

In addition to this, preliminary data from the McDonald laboratory has suggested a role for another ion channel, the epithelial sodium channel (ENaC), in EMT. The expression of α-ENaC, β-ENaC, and γ-ENaC mRNA was compared between pre-EMT epithelial breast cancer cell lines and post-EMT mesenchymal breast cancer cell lines. They found that α-ENaC, β-ENaC, and γ-ENaC mRNA expression was higher in the pre-EMT epithelial cell lines compared to the post-EMT mesenchymal cell lines (**Figure 1.1**) (Ware, Cunliffe, and McDonald, unpublished data). This suggests a potential role of ENaC in regulating EMT.

1.3 ENaC

ENaC is a sodium channel and belongs to the ENaC/Degenerin family (Hanukoglu & Hanukoglu, 2016). It is found on many epithelia including kidney, lung, colon, and mammary epithelia among others (Boyd & Náray-Fejes-Tóth, 2007; Hanukoglu & Hanukoglu, 2016). It is a heterotrimer composed of an α-subunit or δ-subunit, a β-subunit, and a γ-subunit (**Figure 1.2**).

These subunits are encoded by SCNN1A, SCNN1D, SCNN1B, and SCNN1G respectively. Each subunit consists of two transmembrane domains, a large extracellular loop, and intracellular N- and C-termini (Hanukoglu & Hanukoglu, 2016). The structure of ENaC was recently resolved using cryo-electron microscopy revealing a heterotrimer arranged in a counter-clockwise manner. Each subunit was described as resembling a hand holding a ball, with palm, knuckle, finger, thumb, and ball domains (Noreng *et al.*, 2018). An interaction between the subunits was observed between the finger domain and the knuckle domain of the adjacent subunit. The pore of the channel is made up of the second transmembrane domain of each subunit. The binding site of amiloride, which inhibits ENaC function, and the G/SxS selectivity filter, which allows for high specificity for sodium ions over potassium ions, are found in close proximity to this pore (Kellenberger & Schild, 2002; Noreng *et al.*, 2018).

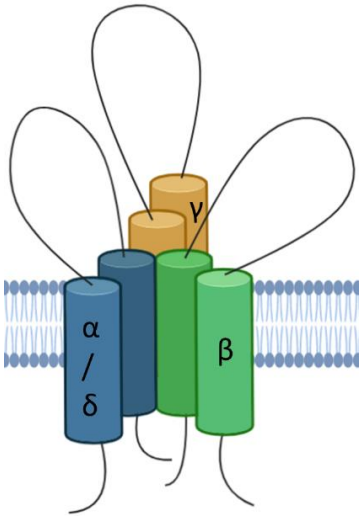

Figure 1.2: Original figure ENaC Structure with an α- or δ-ENaC subunit, a β-ENaC subunit, and a γ-ENaC subunit. Each subunit consists of two transmembrane domains with a large extracellular loop and intracellular terminal domains. Not to scale.

1.3.1 ENaC and Blood Pressure Regulation

An important role of ENaC is in blood pressure regulation. Sodium ions are an important electrolyte involved in extracellular fluid volume. ENaC is found on epithelia of the distal

nephron where it reabsorbs sodium ions, creating an osmotic gradient for water to follow. This process can be regulated by aldosterone. Aldosterone is a mineralocorticoid hormone produced within the adrenal gland (Booth *et al.*, 2002). It has a well characterised role in responding to low blood pressure conditions as part of the Renin-Angiotensin-Aldosterone-System (RAAS) pathway (Booth *et al.*, 2002). Aldosterone binds to the mineralocorticoid receptor (MR) within the principal cells of the cortical collecting duct of the kidney nephron. A rapid response, mediated by the serum and glucocorticoid-regulated kinase 1 (SGK1), increases ENaC activity and ENaC trafficking to the cell surface, and decreases ENaC endocytosis (Loffing *et al.*, 2001; Hermidorff *et al.*, 2017; Valinsky *et al.*, 2018) A later genomic response increases synthesis of ENaC (Verrey, 1995). These result in increased sodium ion reabsorption which provides an osmotic gradient for water reabsorption leading to the expansion of blood volume, and thus an increase in blood pressure back to normal (Hanukoglu & Hanukoglu, 2016; Valinsky *et al.*, 2018). Mutations in the sequence of ENaC lead to dysregulation of blood pressure, resulting in diseases such as Liddle syndrome and Pseudohypoaldosteronism Type 1 (PHA1) (Hanukoglu & Hanukoglu, 2016). Liddle syndrome is characterised by early onset hypertension, hypokalaemia, metabolic alkalosis, low levels of renin and aldosterone. This is caused by a gain of function mutation which leads to an increase in sodium reabsorption (Shimkets, 1994). PHA1 is characterised by salt wasting, hyperkalaemia, and metabolic acidosis. This is caused by a loss of function mutation resulting a reduction in sodium reabsorption (Chang *et al.*, 1996; Strautnieks *et al.*, 1996).

1.3.2 δ-ENaC

The δ-ENaC subunit is encoded by the SCNN1D gene. It is a subunit that is found in humans but not within rodent models and therefore cannot be easily studied. It can replace α-ENaC to form a heterotrimer with β-ENaC and γ-ENaC. The δ-ENaC subunit can be found on both epithelial and non-epithelial tissue, with expression in heart, liver, brain, lung, skeletal muscle, and blood leukocytes compared to αβγ-ENaC, which is predominantly expressed in the kidneys, lungs and liver (Ji *et al.*, 2012). Compared to αβγ-ENaC, δβγ-ENaC shows higher selectivity for sodium ions over lithium ions, is more sensitive to extracellular protons, and less sensitive to inhibition by amiloride (Giraldez *et al.*, 2012; Ji *et al.*, 2012). The function of δ-ENaC is still unknown with some suggestion of roles within the brain, pancreas, and lung (Giraldez *et al.*, 2012).

1.3.3 ENaC and Migration

ENaC has been shown to be involved in cellular migration. A study investigated the role of ENaC in migration of keratinocytes (Yang *et al.*, 2013). They demonstrated that ENaC influences the direction of movement in the presence of an electric field that exist within a wound. ENaC is able to stabilise lamellipodia in the direction of the cathode and leads to directional migration to close the wound (Yang *et al.*, 2013). ENaC has also been shown to be involved in vascular smooth muscle cell (VSMC) migration (Grifoni *et al.*, 2006). ENaC was confirmed to be expressed within two VSMC cell lines, SV40-LT and A10 (Grifoni *et al.*, 2006). The migratory ability of these cells were significantly reduced when ENaC was inhibited by benzamil, or knocked down with siRNA (Grifoni *et al.*, 2006). This suggests that ENaC plays an important role in VSMC migration.

The role of ENaC in migration could be explained by its contribution to cell volume as well as its interaction with the cell cytoskeleton. ENaC may be involved in regulatory volume increase (RVI). When cells are put under hypertonic stress, hypertonicity-induced cation channels are induced to restore cell volume. When ENaC subunits were knocked down in rat hepatocytes, these cells had a reduced RVI response. This suggests that ENaC may be related to these hypertonicity-induced cation channels (Plettenberg *et al.*, 2008). ENaC has also been shown to have direct interactions with the cellular cytoskeleton (Mazzochi *et al.*, 2006). A co-sedimentation assay was performed and showed a direct interaction between the C-terminal domain of α-ENaC and F-actin (Mazzochi *et al.*, 2006). These show ENaC is involved in cell migration. This is possibly due to its role in cell volume or its interaction with the cell cytoskeleton, leading to the formation of cellular protrusions required for cellular migration (Schwab, 2001).

1.3.4 ENaC and Cancer

A number of studies have shown a role for ENaC in cancer (Kapoor *et al.*, 2009; del Mónaco *et al.*, 2009; Yamamura *et al.*, 2008; Amara *et al.*, 2016). Due to their location on the cell surface, ion channels such as ENaC are accessible targets for potential treatments of cancer (Prevarskaya *et al.*, 2018). ENaC and acid sensing ion channel 1 (ASIC1), members of the ENaC/Degenerin superfamily, have been shown to be involved in migration of D54-MG human glioblastoma multiforme cells (Kapoor *et al.*, 2009). D54-MG cells had significantly higher mRNA expression of ASIC1, α-ENaC, and γ-ENaC compared to primary human astrocytes. When these subunits were knocked down, they observed a reduction in migration compared

to the control. Treatment of these cells with an amiloride analogue, benzamil, also lead to a reduction in migration (Kapoor *et al.*, 2009).

Another study looked at the role of ENaC in choriocarcinoma. A study by del Monaco et al, investigated the change in migration of BeWo choriocarcinoma cancer cells using a wound healing assay with aldosterone to increase ENaC activity, and amiloride to inhibit ENaC activity. They observed a significant increase in cell migration when aldosterone was added as compared to the control. Using sense and anti-sense oligonucleotides for α-ENaC, they demonstrated that the increase in migration with aldosterone was due to ENaC. They showed that cells with anti-sense oligonucleotides had decreased migration compared to cells with sense oligonucleotides and no oligonucleotides (del Mónaco *et al.*, 2009). This showed that ENaC has a role in migration in choriocarcinoma cells (del Mónaco *et al.*, 2009).

Another study looking at G-361 melanoma cells suggested the involvement of ENaC in cancer (Yamamura *et al.*, 2008). They demonstrated that all four ENaC subunits were expressed within the G-361 melanoma cells using reverse transcription polymerase chain reaction (RT-PCR), in-situ hybridisation, and immunostaining. Validating the expression of ENaC within these melanoma cells suggests a potential role as a novel target in the treatment of melanoma (Yamamura *et al.*, 2008).

However, there is limited research looking at ENaC in breast cancer. One study suggests ENaC is involved with IL-17 and inflammatory stress in breast cancer cells that aid in tumour proliferation (Amara *et al.*, 2016). High sodium chloride and IL-17 in breast cancer cell lines leads to production of reactive oxygen and nitrogen species. There was increased expression

of the γ-ENaC subunit when the cell was treated with both IL-17 and high sodium chloride. Knock down of γ-ENaC also led to a reduction in the production of reactive oxygen and nitrogen species suggesting that it is involved (Amara *et al.*, 2016). This study shows that ENaC is involved in breast cancer.

A bioinformatics tool, created by Györffy et al, is able to compare the effect of expression levels of genes on breast cancer prognosis (Györffy *et al.*, 2010). Using this bioinformatics tool, SCNN1A and SCNN1D, or α-ENaC and δ-ENaC, were examined (**Figure 1.3**) and the results showed that higher expression of either α-ENaC or δ-ENaC mRNA in breast cancer patients was correlated with a better prognosis. This also suggests a role of ENaC in breast cancer.

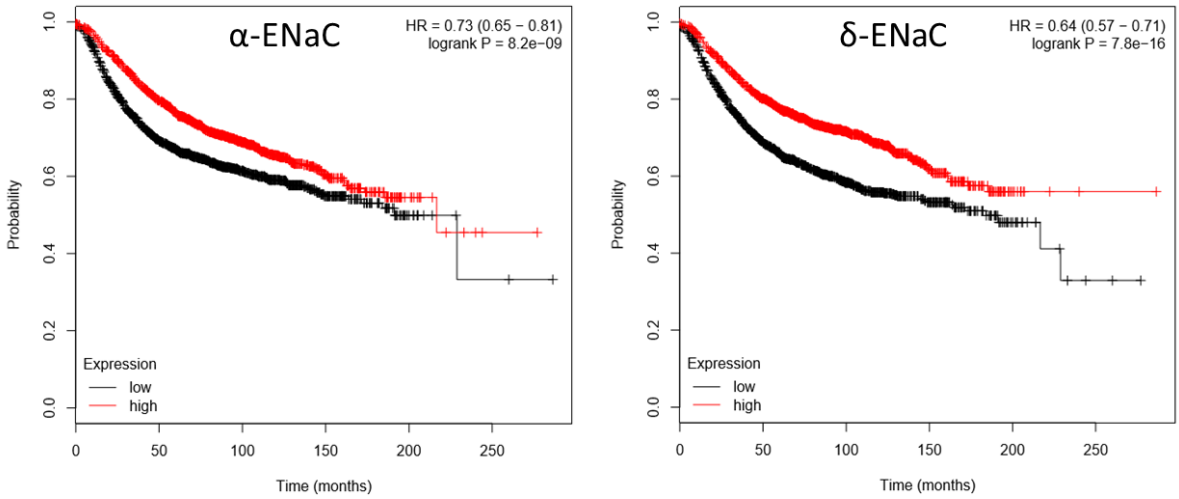

Figure 1.3: Higher expression of α-ENaC or δ-ENaC was correlated with a better prognosis. Carried out by author using bioinformatics tool developed by Györffy et al. The red line represents the prognosis with high expression of the gene of interest and the black line represents the prognosis with low expression of the gene of interest. Left) Comparison of high and low α-ENaC expression with Breast Cancer survival; Right) Comparison of high and low expression of δ-ENaC with Breast Cancer survival.

1.4 Project Rationale

Breast cancer is an important disease around the world. Almost 700 deaths occur each year in New Zealand, with a majority of breast cancer deaths due to metastases. Current treatments

for metastatic breast cancer are limited so identifying novel targets could potentially reduce the burden of disease. EMT has been shown to be important in cancer progression into a metastatic disease, with ion channels being identified as important regulators of EMT. Preliminary data from the McDonald laboratory suggests that ENaC may be involved in EMT, as ENaC mRNA levels is higher in epithelial-like breast cancer cell lines compared to mesenchymal-like breast cancer cell lines. While ENaC plays a vital role in blood pressure regulation, a role of ENaC in cell migration has also been shown. ENaC has also been demonstrated to be involved in many different cancers including glioblastoma, choriocarcinoma, melanoma, and breast cancer, with bioinformatics data suggesting that higher expression of ENaC mRNA improves the prognosis of breast cancer patients. A previous honours student from the McDonald Laboratory explored the role of ENaC in breast cancer cell migration with the use of aldosterone to upregulate ENaC expression, and amiloride to inhibit ENaC function. Scratch assays and Boyden Chamber assays were conducted to observe whether migration was affected by the different conditions. McQueen (2018), found that amiloride could significantly reduce migration in scratch assays in two breast cancer cell lines, while aldosterone was able to increase migration in one breast cancer cell line but reduced migration in another (McQueen, 2018). This shows that ENaC may be involved in breast cancer cell migration, but more specific up and down regulation of ENaC is required to build on these results.

1.5 Aims and Hypothesis

The aim of this project was to understand the role of ENaC, specifically α-ENaC and δ-ENaC, in breast cancer cell migration. To do this α-ENaC or δ-ENaC were overexpressed or knocked

down within two breast cancer cell lines. Scratch assays were performed as a functional test for breast cancer cell migration and qPCR was performed to validate whether successful transfection has occurred.

My hypotheses were that:

“Overexpression of α-ENaC or δ-ENaC in mesenchymal breast cancer cells would lead to an increase in migration”

and

“Knockdown of α-ENaC or δ-ENaC in mesenchymal breast cancer cells would lead to a decrease in migration”.

2 Methods and Materials

2.1 Cells

For this project, two triple negative mesenchymal breast cancer cell lines: MDA-MB-231 and BT-549 cells were obtained from Dr Heather Cunliffe (Department of Pathology, University of Otago). Cell stocks were grown on 6cm cell culture plates (Falcon, Cat. No. 353002, Corning, USA) and incubated at 37˚C with 5.5% CO_2 in a Forma Series II incubator (Thermo Electron Corporation). All experiments were performed in Physical Containment 2 laboratories.

2.1.1 MDA-MB-231

MDA-MB-231 cells are a triple negative, mesenchymal breast cancer cell line originating from the pleural effusion of a Caucasian female (**Figure 2.1A**). These cells were grown in filtered (Corning, Cat. No. COR430513, USA) RPMI-1640 media (Gibco, Cat. No. 31800-022, Thermo Fisher Scientific, USA) supplemented with 2g/L of glucose, 1.5g/L of sodium bicarbonate, 10% Foetal Bovine serum (FBS) (Gibco, Cat. No. 10091-155, Thermo Fisher Scientific, USA), and 1% penicillin streptomycin (Gibco, Cat. No. 15140-122, Thermo Fisher Scientific, USA).

2.1.2 BT-549

BT-549 cells are another triple negative, mesenchymal breast cancer cell line originating from the mammary gland of a Caucasian female (**Figure 2.1B**). These cells were grown in filtered RPMI-1640 media supplemented with 4.5g/L of glucose, 1.5g/L of sodium bicarbonate, 110.04mg/L of sodium pyruvate, 2383mg/L of HEPES, 800 µL/L of insulin-transferrin-selenium (Gibco, Cat. No. 41400045, Thermo Fisher Scientific, USA), 10% FBS, and 1% penicillin streptomycin.

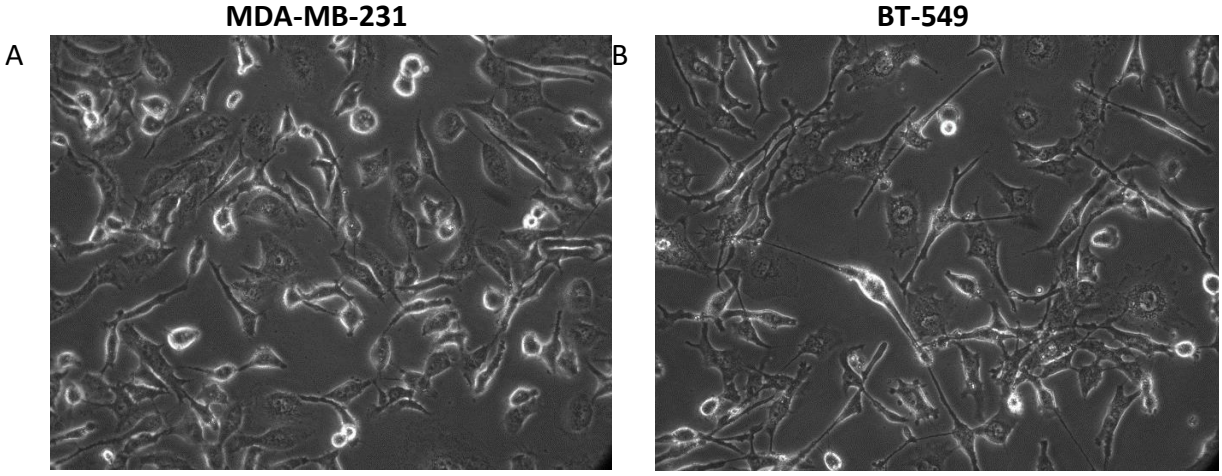

Figure 2.1: Images of the two cell lines used in this project. A) MDA-MB-231 Cells; B) BT-549 Cells. Viewed under 20x magnification using an Olympus CKX41 microscope.

2.2 Cell Passaging

MDA-MB-231 and BT-549 cells were passaged twice a week to ensure healthy growth of the cells and to limit cell death due to overcrowding. This was carried out in a sterile biological safety cabinet (Class II Type A2, Labconco) to minimise the chance of infection of the cells. The cell media was removed using a vacuum with a sterile pipette tip attached. The cells were subsequently washed using filtered phosphate-buffered saline (PBS) (Gibco, Cat. No. 18912-014, Thermo Fisher Scientific, USA) to remove any dead cells. The PBS was then removed and ~500µL of 0.25% Trypsin/ 1mM EDTA (Gibco, Cat. No. 25200-056, Thermo Fisher Scientific, USA) was pipetted onto the plate. The plate was incubated for ~5 minutes, then 1mL of cell specific media was added to neutralise the trypsin and the cells were resuspended by gentle pipetting. From here the cells can be counted (Section 2.3) or directly seeded onto a new plate. A new 6cm cell culture plate had 4mL of cell media pipetted onto it and ~400µL of media containing approximately 400,000 resuspended cells was pipetted drop-wise around the plate. The plate was then labelled with my name, date, cell line, and passage number, with the

passage number increasing by one from the previous plate. This was placed into the 37˚C + 5.5% CO_2 incubator until confluence was reached again in approximately 3 days.

2.3 Cell Counting

Similar steps to cell passaging (Section 2.2) were performed to lift the cells off the plate. The cell containing solution was transferred into a 15mL tube (Greiner Bio-One, Cat. No. 188261, Greiner, Germany) and centrifuged (Eppendorf, Centrifuge 5702) for 3 minutes at 3 revolutions per minute (RPM). The cell media was then removed and the cell pellet was resuspended in 1mL of media. A volume of 10µL was pipetted onto a haemocytometer (Marienfeld, Cat. No. 0680010, Germany) and the number of cells within a 5X5 grid was counted (n) using the 10X objective on a microscope (Olympus, CKX41). This gives a concentration of cells at $nx10^4$/mL. The solution with the known number of cells can then be used to seed a specific number of cells onto a plate using the $\mathbf{c_1v_1 = c_2v_2}$ formula.

2.4 Scratch Assay

The scratch assay or wound healing assay was performed to quantify the ability of a cell to migrate (Hulkower & Herber, 2011). A scratch was made on a monolayer of cells where nearby cells can infiltrate. Photographs were taken at specific time points to observe changes in the size of the scratch area due to migration. This was conducted over a 24h period therefore the decrease in scratch area was likely due to cellular migration rather than proliferation. Each condition was repeated until at least four biological repeats (N), using cells with different passage numbers, and four total experimental repeats (n) was reached.

2.4.1 Cell Seeding

Cells were counted following the method from the cell counting section (Section 2.3). A volume containing 300,000 cells was calculated and pipetted drop-wise onto one well of a six-

well plate (Greiner Bio-One, Cat. No. GRE657160, Greiner, Germany) containing 2mL of media. This was repeated for the five remaining wells. These wells were left for approximately one day to form a confluent monolayer, at which point transfection could occur. Each cell line was put into separate rows of the six-well plate, with each column having a different experimental condition (**Figure 2.2**).

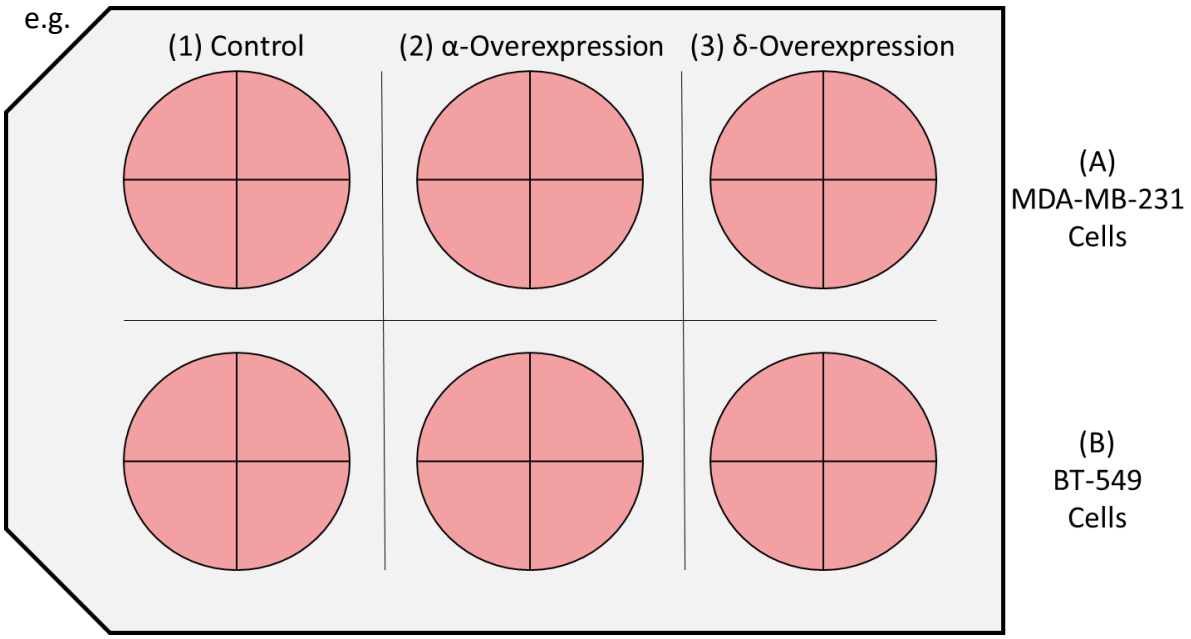

Figure 2.2: Experimental set-up for the Scratch Assays using a six-well plate. Each row contains the same cell-line e.g. MDA-MB-231 in row A and BT-549 in row B. Each column contains the same condition e.g. Control in column 1, α-ENaC overexpression in column 2, and δ-ENaC overexpression in column 3.

2.4.2 Cell Transfection

Cell transfection is a technique that allows the uptake of genetic material into cells. This was performed to understand the role of specific proteins by modifying their expression and observing the resultant phenotype. In this project, transfection was achieved using the Lipofectamine 3000 Transfection reagent (Invitrogen, Cat. No. L3000015, Thermo Fisher Scientific, USA).

Cells seeded onto a plate were left for one day to adhere to the plate and form a confluent monolayer. Two micro-centrifuge tubes (Multi-Max, Cat. No. MUL2942, USA) were required for each transfection. The first micro-centrifuge tube was filled with 50µL of serum-free media and 3µL of Lipofectamine 3000 and incubated for ~5 minutes. The second micro-centrifuge tube was filled with 50µL of serum-free media, 2µL of P3000, and 0.3µg of DNA plasmid, for overexpression experiments, or 20pmol of siRNA, for knockdown experiments, and were vortex mixed. The solution within the second micro-centrifuge tube was transferred to the first micro-centrifuge tube and vortex mixed. This was incubated for ~15 minutes at room temperature to enable formation of liposome complexes. The media, within the six well plate containing cells, was replaced with serum-free media and the transfection solution was added to the plate in a drop-wise fashion evenly around the plate. After six hours, the media was replaced with serum containing media.

2.4.2.1 DNA Plasmid

The DNA plasmids used for overexpression in this project utilised the pMT3 vector which contains an adenovirus major late promoter (Swick *et al.*, 1992). This project used human α-ENaC and δ-ENaC with pMT3 vector and an empty pMT3 vector as the control. Approximately 0.3µg of DNA plasmid was transfected per experiment.

2.4.2.2 siRNA

siRNAs were used to bind to their complementary mRNA, and inhibit translation leading to decreasing protein level. For this project α-ENaC siRNA and δ-ENaC siRNA (Sigma Aldrich, USA) (**Table 2.1**) were used to knockdown α-ENaC and δ-ENaC respectively, with scrambled mouse control siRNA (Dharmacon, Horizon Discovery, USA) used as the control. Approximately

20pmol of siRNA was transfected per experiment. The siRNA complementary binding site can be predicted using the Basic Local Alignment Search Tool (BLAST)

Table 2.1: siRNAs used in this project with their sequence, complementary target sequence position, and manufacturer.

siRNA	Sequence	siRNA Target Position
α-ENaC	GCT CTT TGA CCT GTA CAA A	912bp – 930bp; Exon
δ-ENaC	CAA GTC AGC TGG ATG GAC T	2134bp – 2152bp; Exon

2.4.2.3 Aldosterone

A previous honours project demonstrated that aldosterone was able to alter migration in MDA-MB-231 and BT-549 mesenchymal breast cancer cells (McQueen, 2018). An aldosterone scratch assay was performed as a positive control alongside an α-ENaC overexpression and control scratch assays. The scratch assays were set up as previously described (Section 2.4.1 and 2.4.2.). The control cells and aldosterone cells were transfected with pMT3 empty vector control, while the α-ENaC overexpression cells were transfected with α-ENaC DNA plasmids. The cell monolayers were then scratched and the cell media was replaced to remove any debris (Section 2.4.3). A volume of aldosterone, resulting in a concentration of 10nM, was pipetted drop-wise to the aldosterone well. The same volume of 100% ethanol pipetted drop-wise to the control and α-ENaC wells as a vehicle control.

2.4.3 Scratching Protocol

A glass pipette with a rounded tip was used to scratch the cell monolayer. The glass pipette was sterilised by dipping into 100% ethanol and flaming with a lighter. This was carried out twice before scratching each plate. Light pressure was used to remove the cells off the plate, but not enough to damage the plate. The plate lid was used as a guide for the scratch to be made. An initial vertical scratch was made followed by a second horizontal scratch (**Figure 2.3**)

and a point of reference was added using a permanent marker where the scratches intersect. The plate was then washed with 1mL of PBS to remove any floating or dead cells and full media was added.

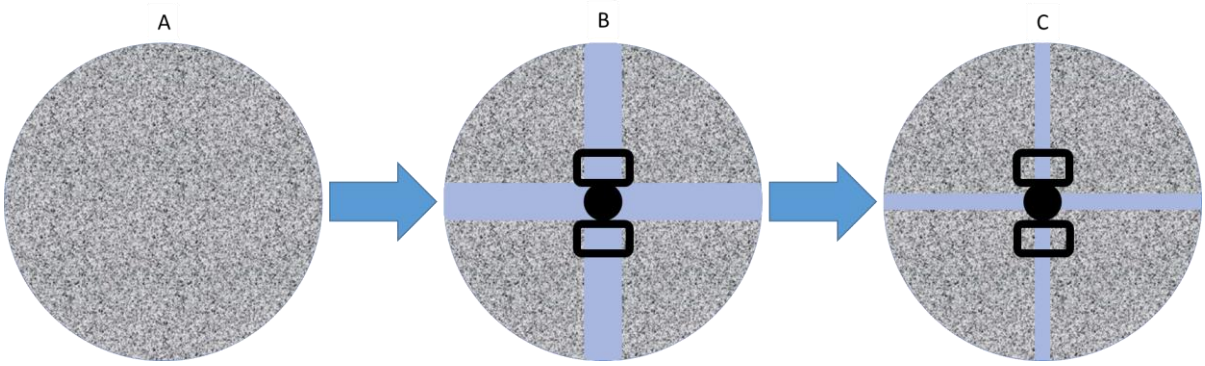

Figure 2.3: Depicts changes to the cell monolayer following scratching of plate and cell migration. A) Monolayer before the Scratch; B) Scratch at 0 hours; C) Scratch at 12 hours. Black rectangles represent the area captured in the photograph.

2.4.4 Photograph

Photographs of the scratch area were taken with a microscope with the 10X objective (Olympus U-RFLT50) using an Infinity 3-1UM microscope camera and Infinity Capture software (Teledyne Lumenera, Canada). The photographs were taken at seven time points: 0, 1, 3, 5, 8, 12, and 24 hours after the scratch. Two photographs were taken of each plate, at each time point, capturing the same scratch area relative to the reference point (**Figure 2.4**). The photographs captured were analysed using Image J (Version 1.52n, NIH, USA) with an MRI Wound Healing Tool Macro (Montpellier RIO Imaging, CNRS, Montpellier, France). The options were set to Method: Variance, 10 for "Variance Filter Radius", 40 for "Threshold", 6 for "Radius Open", and 10000 for "Minimum Size". The photographs were first processed in Image J by first smoothing the image, followed by enhancing contrast by 0.3%. The scratch area of the two photographs was averaged and a percentage of the initial scratch area was calculated.

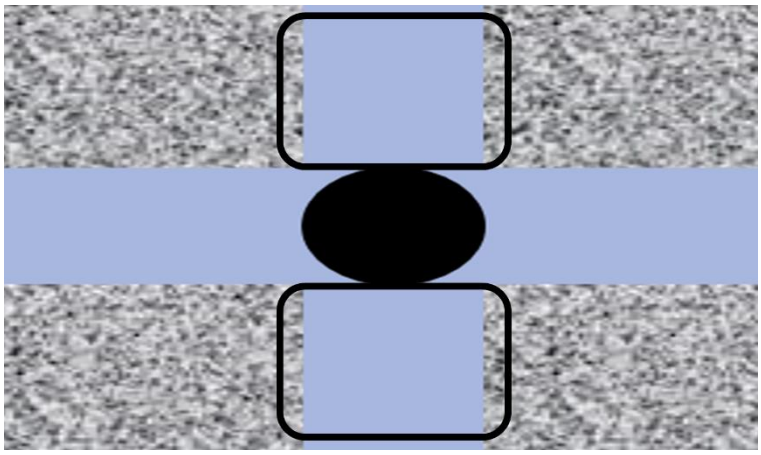

Figure 2.4: Two photographs were captured at each time point for each plate. The black rectangles represent the area captured for analysis by the photographs.

2.4.5 Cell Lysis

After the last photograph was taken at 24 hours after the scratch, the cells were lysed and the lysate was collected for quantitative polymerase chain reaction (qPCR). The media was removed and the plate was washed with PBS. To lyse the cells, 300µL of TRIzol reagent (Invitrogen, Cat. No. 15596026, Thermo Fisher Scientific, USA) was added to the plate, and incubated for ~5 minutes. The cell lysates were collected and transferred to micro-centrifuge tubes. These were labelled and stored in a -80˚C freezer until it was ready for RNA extraction.

2.5 RNA Extraction

RNA extraction was performed using the "RNeasy Micro Kit" (Qiagen, Cat. No. 74004, Germany) following the "TGen BOCRU RNA Micro Prep Extraction w/Qiagen RNeasy Kit" protocol by C. Mancini (Section 6.1). Cell lysates were thawed and 40µL of chloroform added. This separated the cell lysates into an upper aqueous layer containing RNA, and a lower organic layer containing DNA and proteins. The aqueous layer was collected and underwent a series of washing and centrifugation steps using the Qiagen Micro-RNeasy Column. This resulted in 20µL of extracted RNA and the concentration of this RNA was quantified using a microplate reader (BioTek, Synergy 2).

2.6 Reverse Transcription

Complementary or Template DNA (cDNA) was required for PCR and was synthesised by performing reverse transcription with extracted RNA (Section 2.5). This was carried out using the "PrimeScript RT Reagent Kit" (Takara, Cat. No. RR037A, Japan). Reverse transcription was performed by adding to a micro-centrifuge tube: 2µL of 5x Primescript buffer, 0.5µL of reverse transcriptase enzyme, 0.5µL of Oligo dT primer, 0.5µL of random hexamers, extracted RNA, and water to a total of 10µL. Each reaction required RNA at a final concentration of 50ng/µL which was calculated using the known RNA concentration. This was incubated at 37˚C for 15 minutes. The reverse transcriptase enzyme was then inactivated by incubating samples at 85˚C for 5 seconds and 40µL of water was added to dilute the cDNA 5x, resulting in 50µL of cDNA that was ready for qPCR.

2.7 Quantitative Polymerase Chain Reaction

Quantitative polymerase chain reaction (qPCR) was conducted to determine whether transfection of plasmid DNA or siRNA was successful. This was performed on a 96-well plate (Multi-Max, Cat. No. MUL3890, USA) with each experimental condition carried out in triplicate per gene of interest and then the plate was sealed (Excel Scientific, Cat. No. EXCTS-RT2RR-100, USA). Each well contained 10µL of solution consisting of 5µL of SYBR with ROX (Takara, Cat. No. RR420L, Japan), 3.6µL of water, 0.2µL of forward primer, 0.2µL of reverse primer, and 1µL of cDNA.

2.7.1 Primers

The primers used in my experiment were: α-ENaC, δ-ENaC, and GAPDH (Sigma Aldrich, USA) (**Table 2.2**). The PCR product sizes were predicted using BLAST (National Center for Biotechnological Information, 2019).

Table 2.2: Primers used in this project with their sequence, manufacturer, and the predicted PCR product size.

Primer	Sequence	PCR Product Size
GAPDH Forward Primer	ACAGTTGCCATGTAGACC	88bp
GAPDH Reverse Primer	TTGAGCACAGGGTACTTTA	
α-ENaC Forward Primer	GGGTACTGCTACTATAAGCTC	185bp
α-ENaC Reverse Primer	TTGACGGTGTAATTGTTCTG	
δ-ENaC Forward Primer	AGGGAGTCTGCATTCAAG	143bp
δ-ENaC Reverse Primer	GATGTTGATTTTGGCCAGG	

2.7.2 Cycle

The qPCR cycle protocol was designed by Dr Adam Ware from the McDonald Lab and was conducted using Bio-Rad's CFX Connect Real-Time System. The steps of the protocol are as outlined in Table 2.3.

Table 2.3: Steps with corresponding action featuring temperature and time

Step	Action
1	95˚C for 10 minutes
2	95˚C for 15 seconds
3	60˚C for 1 minute
4	Repeat Steps 2-3 40 times
5	65˚C for 15 seconds
6	95˚C for 30 seconds

2.7.3 Fold Change Calculation

To determine the magnitude of the change in mRNA expression with overexpression and knockdown, a fold change calculation was carried out using the $\mathbf{2^{-\Delta\Delta CT}}$ equation. This calculated the fold change relative to the experimental control, normalised with the GAPDH housekeeping gene, using the difference in PCR cycle times.

2.7.4 Agarose Gel Electrophoresis

To determine whether the primers produced the correct PCR product, agarose gel electrophoresis was performed. Agarose gel electrophoresis can approximate the size of PCR products, based on the position of the band on the gel relative to a ladder after completion. A 2.5% agarose gel was made by combining 1.5g of agarose (Bioline, Cat. No. BIO-41025, United Kingdom) with 60mL of 1x TAE Buffer. This was microwaved until it boiled and the solution became transparent. This was left to cool for ~5 minutes at which point 5µL of SYBR safe DNA gel stain (Invitrogen, Cat. No. S33102, Thermo Fisher Scientific, USA) was added. The solution was then carefully poured into a gel mould and left to set for ~15 minutes. During this time, the PCR products were prepared. Experimental and water control triplicates were chosen and the triplicates were pooled together with 2µL of gel loading dye (New England Biolabs, Cat. No. B7025S, USA). The experimental triplicate contained cDNA and primers while the water control triplicate contained water and primers. In an empty well 2µL of gel loading dye was mixed with 0.7µL of the ladder solution (New England Biolabs, Cat. No. N3200S, USA). When the gel had set, it was placed into the running chamber (Bio-Rad, Wide Mini-Sub Cell GT Cell) and submerged in 1x TAE buffer, with the gel oriented so the wells were closest to the negative electrode. The wells were loaded with the ladder loaded into the leftmost well followed by each pair of experimental and water control triplicates. The agarose gel electrophoresis was run at a constant voltage of 100V, 3A, and 300W for 30 minutes (Select BioProducts, BioVolt 250V). Once this was complete, the gel could be imaged (Syngene, PXi). The size of the PCR products could be estimated using its position relative to the ladder. This could be compared with the predicted size of the PCR products.

2.8 Statistical Analysis

2.8.1 Two-way ANOVA

A two-way ANOVA with Tukey's post hoc test was performed to identify any statistically significant differences in the cell migration from the scratch assays. This was carried out using Prism 7 and identified whether there was a difference in the means of each condition at each time point. A P-value of less than 0.05 was considered a statistically significant difference.

2.8.2 Student's T-Test

Unpaired Student's T-Tests with Welch's correction for unequal variance were performed to identify whether there was a significant difference in the mean relative fold change of α-ENaC mRNA or δ-ENaC mRNA, when these were overexpressed or knocked down, compared to the control. This was carried out using Prism 7 to determine whether overexpression with plasmid DNA transfection, or knockdown with siRNA transfection, was successful. A P-value of less than 0.05 was considered a statistically significant difference.

3 Results

This project aimed to understand the role of α-ENaC and δ-ENaC in breast cancer cell migration. To do this, α-ENaC or δ-ENaC were either overexpressed or knocked down in two mesenchymal breast cancer cell lines: MDA-MB-231 and BT-549. The migratory ability of these cells was assessed with the use of scratch assays. Photographs were taken of the scratch area at seven time points: 0, 1, 3, 5, 8, 12, and 24 hours after the scratch. As the cells migrate into the scratch area, the area that remained uncovered by cells at each time point decreased. The uncovered area at each time point was quantified, using the MRI wound healing macro on Image J, as a percentage of the original scratch area. These experiments were repeated until each experimental condition achieved at least four biological (N) repeats, with cells of different passage numbers, and four total experimental (n) repeats. The area at each time point was averaged and the results were plotted on a graph with time in hours on the X axis and scratch area as a percentage of the original scratch area on the Y axis. The cells were then lysed and qPCR was performed to validate whether transfection was successful. These results were represented as the fold change relative to the control. My hypotheses were that overexpression of α-ENaC or δ-ENaC will cause an increase in migration of mesenchymal breast cancer cells and knockdown of α-ENaC or δ-ENaC will cause a decrease in migration of mesenchymal breast cancer cells.

3.1 Effect of altering α-ENaC and δ-ENaC in MDA-MB-231 cells

3.1.1 MDA-MB-231 α-ENaC and δ-ENaC Overexpression

The role of ENaC in breast cancer cell migration was initially investigated in MDA-MB-231 mesenchymal breast cancer cells. MDA-MB-231 cells were transfected with DNA plasmids to overexpress either α-ENaC or δ-ENaC, or with a control plasmid with cell migration being compared using scratch assays (**Figure 3.1**). At 12 hours post-scratch, the mean percentage of the scratch area uncovered by cells for the control was 30.9%, 30.0% for α-ENaC overexpression, and 35.4% for δ-ENaC overexpression (**Figure 3.1B, D, F**). A two-way ANOVA with Tukey's post hoc test was performed and reported no statistically significant differences between α-ENaC overexpression and control, or δ-ENaC overexpression and control at any time point. This suggests that overexpression of α-ENaC or δ-ENaC in MDA-MB-231 cells had no effect on cell migration (N=8; n=12) (**Figure 3.1G**) thus contradicting the hypothesis that overexpression of α-ENaC or δ-ENaC will cause an increase in migration of mesenchymal breast cancer cells.

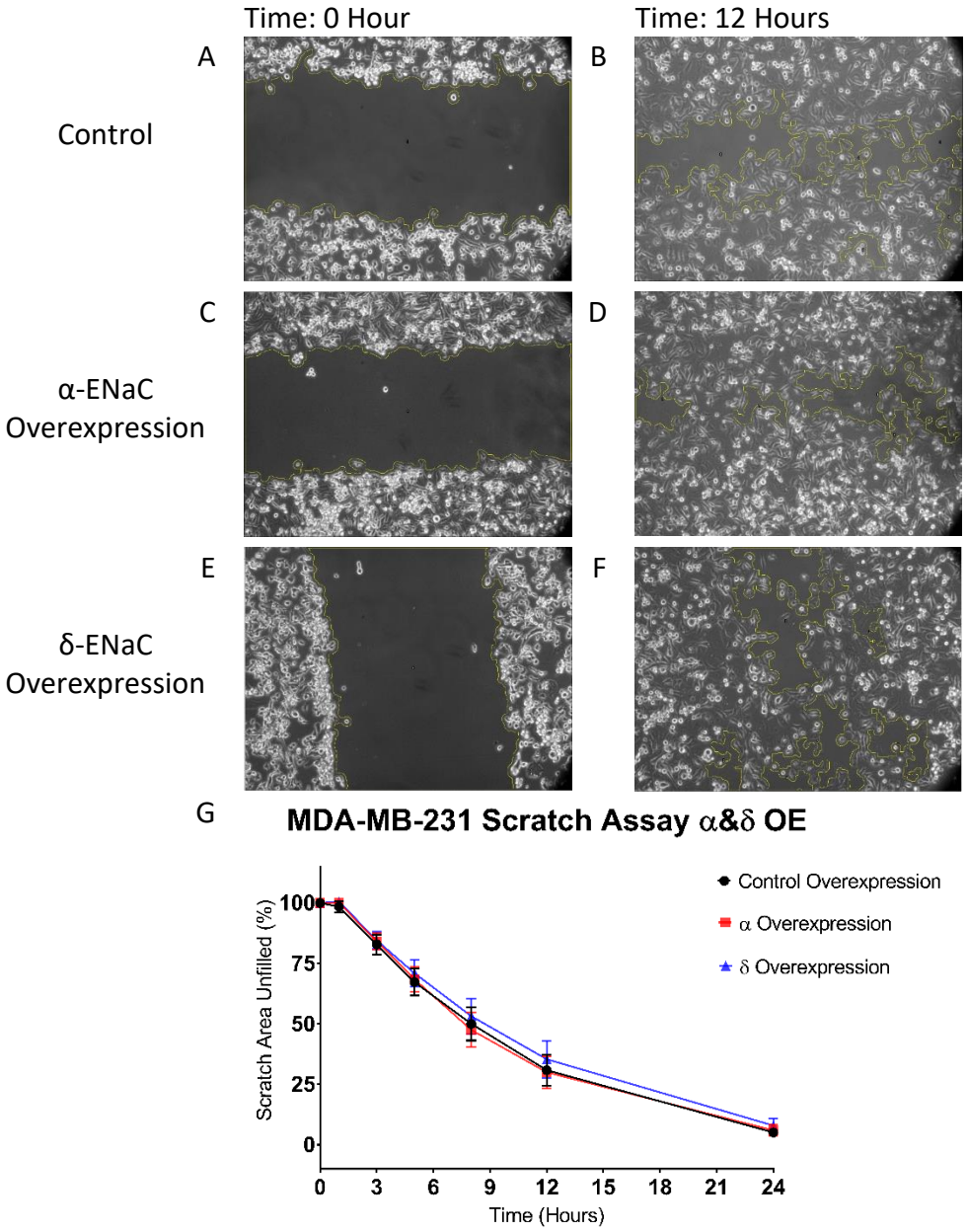

Figure 3.1: The migration of MDA-MB-231 cells, in scratch assays, showed no difference when either α-ENaC or δ-ENaC was overexpressed, compared to the control. A) Control scratch area at time of scratch (0 hours); B) Control scratch area at 12 hours after the scratch (12 Hours); C) α-ENaC overexpression scratch area at time of scratch (0 hours); D) α-ENaC overexpression scratch area at 12 hours after the scratch; E) δ-ENaC overexpression scratch area at time of scratch (0 hours); F) δ-ENaC overexpression scratch area at 12 hours after scratch; G) Pooled results comparing the migratory ability of MDA-MB-231 cells with α-ENaC overexpression and δ-ENaC overexpression to control. Mean ±SEM. Analysed using a two-way ANOVA with Tukey's post hoc test. No statistically significant differences were observed between α-ENaC overexpression and control or δ-ENaC overexpression and control. N=8, n=12.

To determine whether this was due to unsuccessful transfection of plasmids encoding either α-ENaC or δ-ENaC, qPCR was performed using RNA extracted from cells used in the scratch assays described above. The qPCR results showed the mean fold change of α-ENaC mRNA when α-ENaC was overexpressed, was approximately a 13-fold increase relative to the control (N=5) (**Figure 3.2A**). This was not a statistically significant difference when analysed using an unpaired t-test with Welch's correction (P=0.10). This was trending toward statistical significance and was likely due to the large variation in the size of the fold change as every experiment had an increase of at least 4-fold relative to the control. When δ-ENaC was overexpressed, an approximately 4-fold mean increase in δ-ENaC mRNA was shown relative to the control (N=5) (**Figure 3.2B**). There was a statistically significant difference compared to the control (P=0.03), when analysed using an unpaired t-test with Welch's correction. Therefore, overexpression of α-ENaC or δ-ENaC in MDA-MB-231 cells was successful. This suggests that overexpression of α-ENaC or δ-ENaC does not influence migration of MDA-MB-231 breast cancer cells.

To confirm whether the primers were producing the correct PCR product, agarose gel electrophoresis was performed. GAPDH, α-ENaC, and δ-ENaC primers were used in this project and were run alongside a water control. Using the basic local alignment search tool (BLAST), the size of the product was predicted and compared with the position of the band relative to the ladder. The PCR product size of GAPDH was 88bp, 185bp for α-ENaC, and 143bp for δ-ENaC. The DNA gel showed a single band at the correct position and so the primers correctly amplified the specific PCR product (**Figure 3.3**).

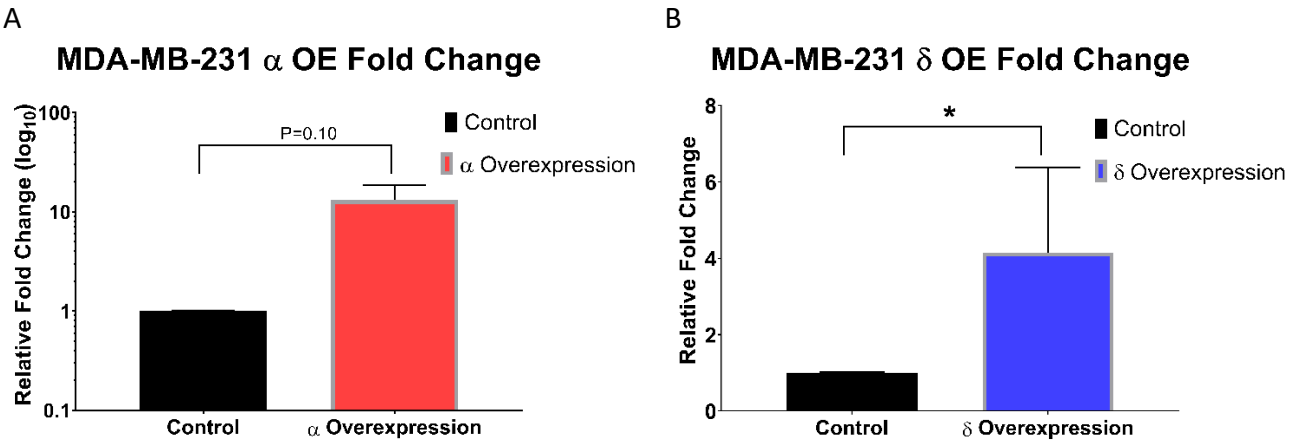

Figure 3.2: Overexpression of α-ENaC or δ-ENaC in MDA-MB-231 cells. A) α-ENaC overexpression had an approximately 13-fold mean increase in α-ENaC mRNA relative to the control. Mean ±SEM. This was trending toward a statistically significant difference when analysed using an unpaired t-test with Welch's correction. P=0.10, N=5, n=9. B) δ-ENaC overexpression had an approximately 4-fold mean increase in δ-ENaC mRNA relative to the control. This was found to be statistically significant when analysed using an unpaired t-test with Welch's correction. *P=0.03, N=5, n=9.

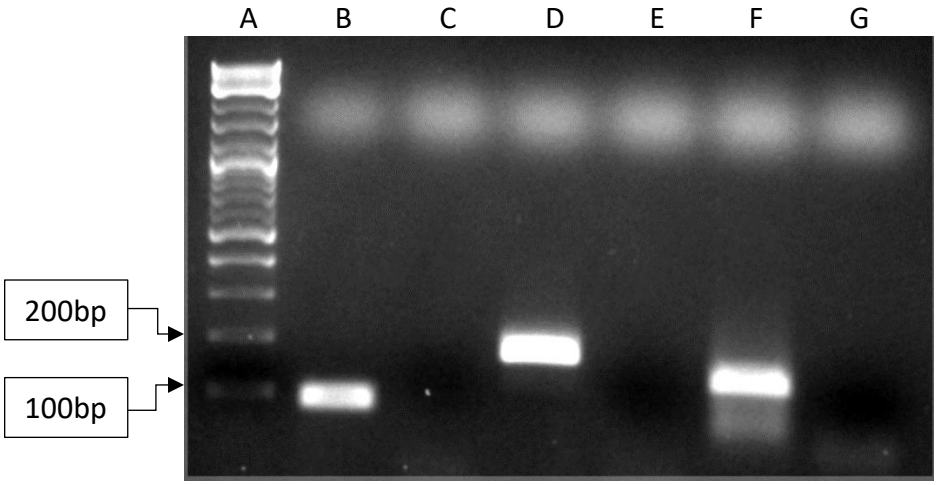

Figure 3.3: Agarose gel electrophoresis confirmed the amplification. A) Ladder; B) GAPDH PCR product; C) GAPDH water control; D) α-ENaC PCR Product; E) α-ENaC water control; F) δ-ENaC PCR product; G) δ-ENaC water control.

3.1.2 MDA-MB-231 α-ENaC and δ-ENaC Knockdown

As the overexpression of α-ENaC or δ-ENaC does not influence the migration of MDA-MB-231 cells, the role of ENaC in breast cancer cell migration was investigated further by observing the effect of lowering α-ENaC and δ-ENaC expression. MDA-MB-231 cells were transfected with siRNA to knockdown either α-ENaC, δ-ENaC, or with a control siRNA. Cell migration was compared using scratch assays (**Figure 3.4**). At 12 hours post-scratch, the mean percentage of the scratch area unfilled for the control was 33.5%, 37.2% for α-ENaC knockdown, and 43.4% for δ-ENaC knockdown (**Figure 3.4B, D, F**). A two-way ANOVA with Tukey's post hoc test was performed and this reported no statistically significant differences between α-ENaC knockdown and control or δ-ENaC knockdown and control at any time point (N=5; n=5) (**Figure 3.4G**). Therefore, knockdown of α-ENaC or δ-ENaC in MDA-MB-231 cells had no effect on cell migration. This contradicted the hypothesis that knockdown of α-ENaC and δ-ENaC will cause a decrease in migration of mesenchymal breast cancer cells.

To validate whether transfection of siRNAs was successful, qPCR was performed using RNA extracted from cells used in the scratch assays described above. When α-ENaC was knocked down, there was an approximate 1.5-fold increase in α-ENaC mRNA relative to the control (N=3) (**Figure 3.5A**). This was not a statistically significant difference (P=0.42), when analysed using an unpaired t-test with Welch's correction. When δ-ENaC was knocked down, an approximate 1.1-fold decrease in δ-ENaC mRNA was shown relative to the control (N=3) (**Figure 3.5B**). There was not a statistically significant difference compared to the control (P=0.44) when analysed using an unpaired t-test with Welch's correction, suggesting that the

knockdown of α-ENaC and δ-ENaC in MDA-MD-231 cells was unsuccessful. This could explain why no effect in migration was observed in these cells when conducting scratch assays.

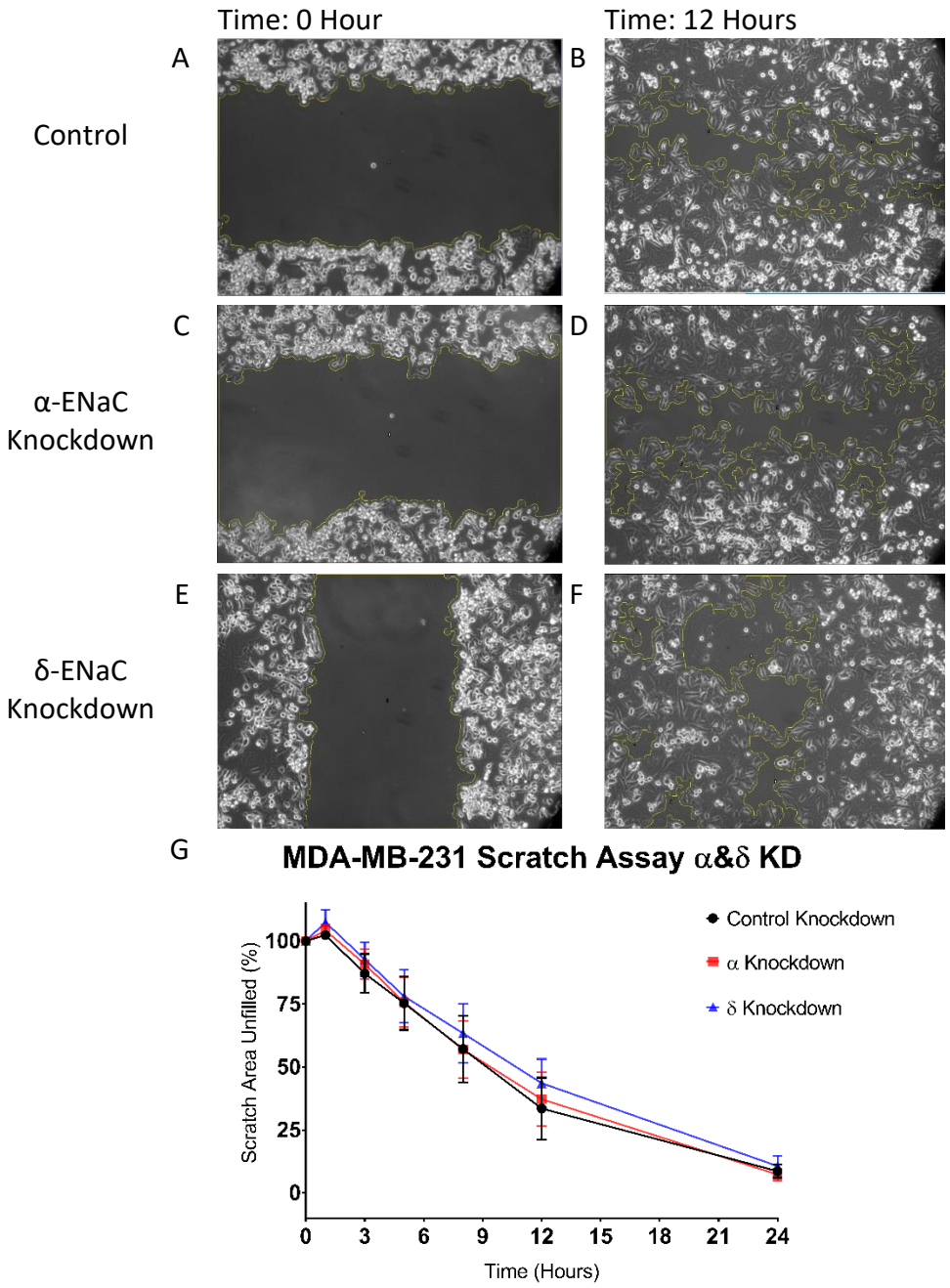

Figure 3.4: The migration of MDA-MB-231 cells, in scratch assays, showed no difference when α-ENaC or δ-ENaC was knocked down, compared to the control. A) Control scratch area at time of scratch (0 Hour); B) Control scratch area at 12 hours after the scratch (12 Hours); C) α-ENaC knockdown scratch area at time of scratch (0 Hour); D) α-ENaC knockdown scratch area at 12 hours after the scratch (12 Hours); E) δ-ENaC knockdown scratch area at time of scratch (0 Hour); F) δ-ENaC knockdown scratch area at 12 hours after scratch (12 Hours); G) Pooled results comparing the migratory ability of MDA-MD-231 cells with α-ENaC knockdown and δ-ENaC knockdown to control. Mean ±SEM. Analysed using a two-way ANOVA with Tukey's post hoc test. No statistically significant differences were observed between α-ENaC knockdown and control or δ-ENaC knockdown and control. N=5, n=5.

A

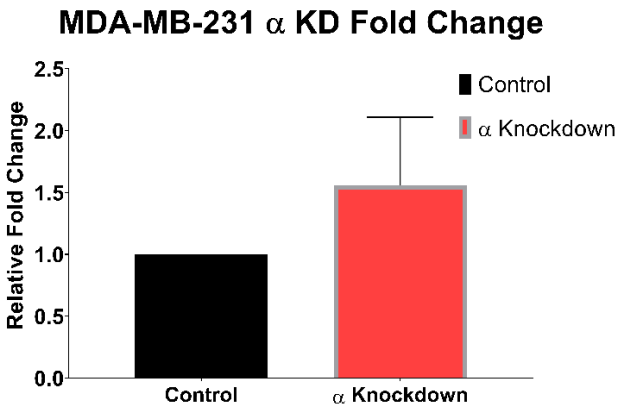

B

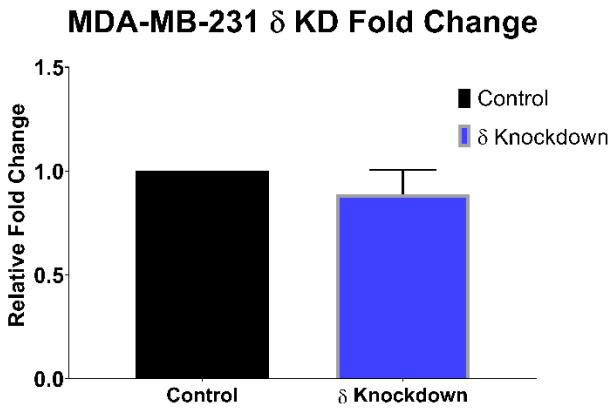

Figure 3.5: Knockdown of α-ENaC or δ-ENaC in MDA-MB-231 cells. A) α-ENaC knockdown had an approximately 1.5-fold mean increase in α-ENaC mRNA relative to the control. Mean ±SEM. This was not a statistically significant difference when analysed using an unpaired t-test with Welch's correction. P=0.42, N=3, n=3. B) δ-ENaC knockdown had an approximately 1.1-fold mean decrease in δ-ENaC mRNA relative to the control. This was not statistically significant when analysed using an unpaired t-test with Welch's correction. P=0.44, N=3, n=3.

3.2 Effect of altering α-ENaC and δ-ENaC in BT-549 cells

3.2.1 BT-549 α-ENaC and δ-ENaC Overexpression

The role of ENaC in breast cancer cell migration was then investigated in another mesenchymal breast cancer cell line, BT-549. BT-549 cells were transfected with DNA plasmids to overexpress either α-ENaC, δ-ENaC, or with control plasmid and cell migration was compared using scratch assays (**Figure 3.6**). At 12 hours post-scratch, the mean percentage of the scratch area unfilled for the control was 35.8%, 39.7% for α-ENaC overexpression, and 39.8% for δ-ENaC overexpression (**Figure 3.6B, D, F**). A two-way ANOVA with Tukey's post hoc test was performed and this reported no statistically significant differences at any time points between α-ENaC overexpression and control or δ-ENaC overexpression and control (N=4; n=6) (**Figure 3.6G**). Therefore, overexpression of α-ENaC or δ-ENaC in BT-549 cells had no effect on cell migration. This contradicted the hypothesis that overexpression of α-ENaC and δ-ENaC will cause an increase in migration of mesenchymal breast cancer cells.

qPCR was performed to validate whether successful transfection had occurred using RNA extracted from cells used in the scratch assays described above. This revealed the mean fold change of α-ENaC, when α-ENaC was overexpressed, was approximately 700-fold increase relative to the control (N=4) (**Figure 3.7A**). This was a statistically significant difference (P=0.03), when analysed using an unpaired t-test with Welch's correction. When δ-ENaC was overexpressed, an approximate 8-fold increase in δ-ENaC mRNA was observed relative to the control (N=4) (**Figure 3.7B**). This was a statistically significant difference compared to the control (P=0.002), when analysed using an unpaired t-test with Welch's correction. Overexpression of α-ENaC or δ-ENaC in BT-549 cells was successful suggesting that α-ENaC or δ-ENaC are not involved in BT-549 cell migration.

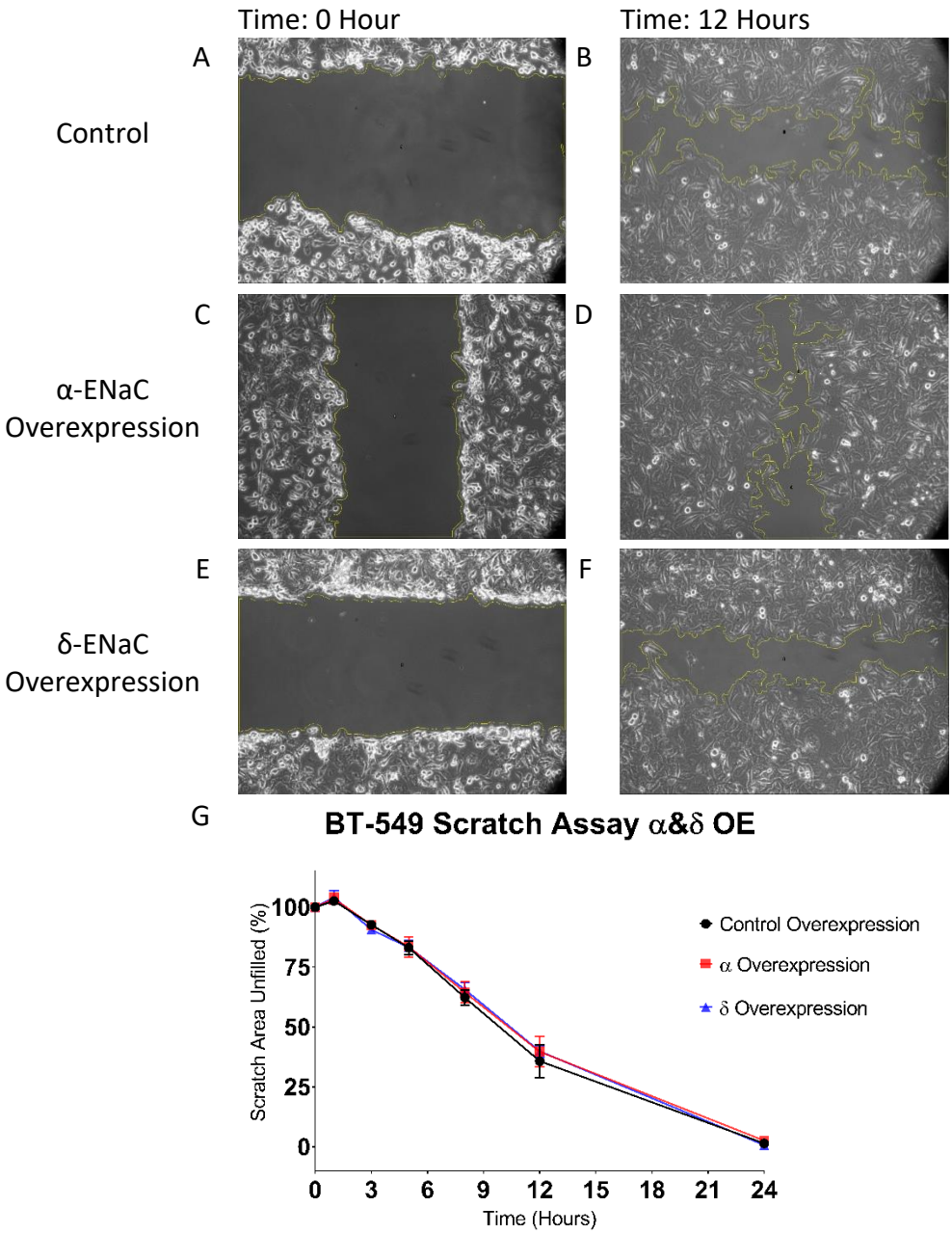

Figure 3.6: The migration of BT-549 cells, in scratch assays, showed no difference when α-ENaC or δ-ENaC was overexpressed, compared to the control. A) Control scratch area at time of scratch (0 Hour); B) Control scratch area at 12 hours after the scratch (12 Hours); C) α-ENaC overexpression scratch area at time of scratch (0 Hour); D) α-ENaC overexpression scratch area at 12 hours after the scratch (12 Hours); E) δ-ENaC overexpression scratch area at time of scratch (0 Hour); F) δ-ENaC overexpression scratch area at 12 hours after scratch (12 Hours); G) Pooled results comparing the migratory ability of BT-549 cells with α-ENaC overexpression and δ-ENaC overexpression to control. Mean ±SEM. Analysed using a two-way ANOVA with Tukey's post hoc test. No statistically significant differences were observed between α-ENaC overexpression and control or δ-ENaC overexpression and control. N=4, n=6.

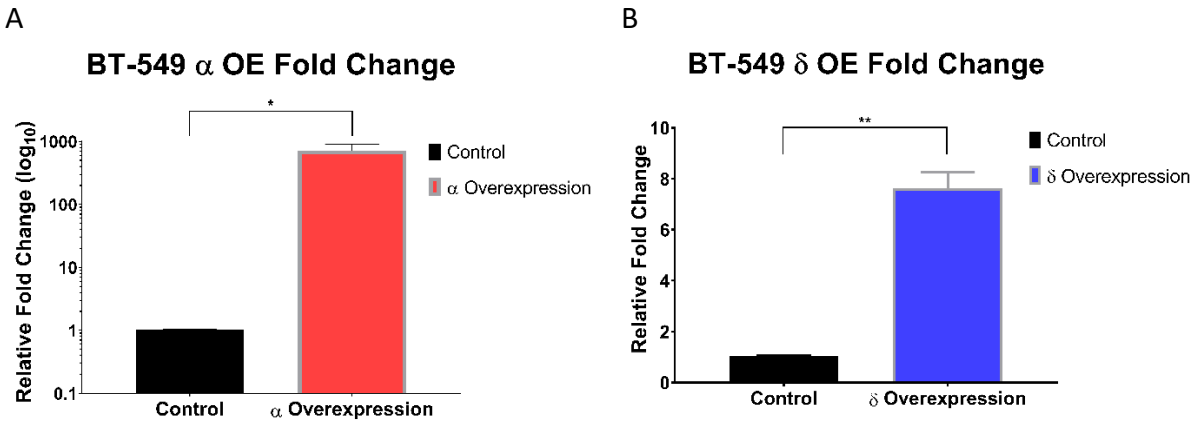

Figure 3.7: Overexpression of α-ENaC or δ-ENaC in BT-549 cells. A) α-ENaC overexpression had an approximately 700-fold mean increase in α-ENaC mRNA relative to the control. Mean ±SEM. This was a statistically significant difference when analysed using an unpaired t-test with Welch's correction. *P=0.03, N=4, n=6. B) δ-ENaC overexpression had an approximately 8-fold mean increase in δ-ENaC mRNA relative to the control. This was found to be statistically significant when analysed using an unpaired t-test with Welch's correction. **P=0.002, N=4, n=6.

3.2.2 BT-549 α-ENaC and δ-ENaC Knockdown

The effect of lowering expression of α-ENaC and δ-ENaC on cell migration was also explored in BT-549 mesenchymal breast cancer cells. BT-549 cells were transfected with siRNA to knockdown either α-ENaC, δ-ENaC, or with a control siRNA. Cell migration was compared using scratch assays (**Figure 3.8**). At 12 hours the mean percentage of the scratch area unfilled for the control was 42.9%, 39.7% for α-ENaC knockdown, and 55.5% for δ-ENaC knockdown (**Figure 3.8B, D, F**). A two-way ANOVA with Tukey's post hoc test was performed and reported no statistically significant differences between α-ENaC knockdown and control or δ-ENaC knockdown and control at any time points (N=4; n=4) (**Figure 3.8G**). Therefore, knockdown of α-ENaC or δ-ENaC in BT-549 cells had no effect on cell migration. This contradicted the hypothesis that knockdown of α-ENaC and δ-ENaC will cause a decrease in migration of mesenchymal breast cancer cells. Interestingly a statistically significant difference in migration was observed between α-ENaC knockdown and δ-ENaC knockdown at 12 and 24 hours after the scratch (P=0.02; P=0.04 respectively) suggesting δ-ENaC may have a role in breast cancer cell migration.

qPCR was performed to validate if transfection was successful using RNA extracted from cells used in the scratch assays described above. When α-ENaC was knocked down, an unexpected approximate mean fold change of 1.7-fold increase was observed in α-ENaC mRNA relative to the control (N=3) (**Figure 3.9A**). This was not a statistically significant difference (P=0.29), when analysed using an unpaired t-test with Welch's correction. Again, when δ-ENaC was knocked down, an unexpected approximate 1.4-fold mean increase in δ-ENaC mRNA was shown relative to the control (N=3) (**Figure 3.9B**). There was no statistically significant difference

compared to the control (P=0.14) when analysed using an unpaired t-test with Welch's correction. Knockdown of α-ENaC and δ-ENaC in BT-549 cells was unsuccessful.

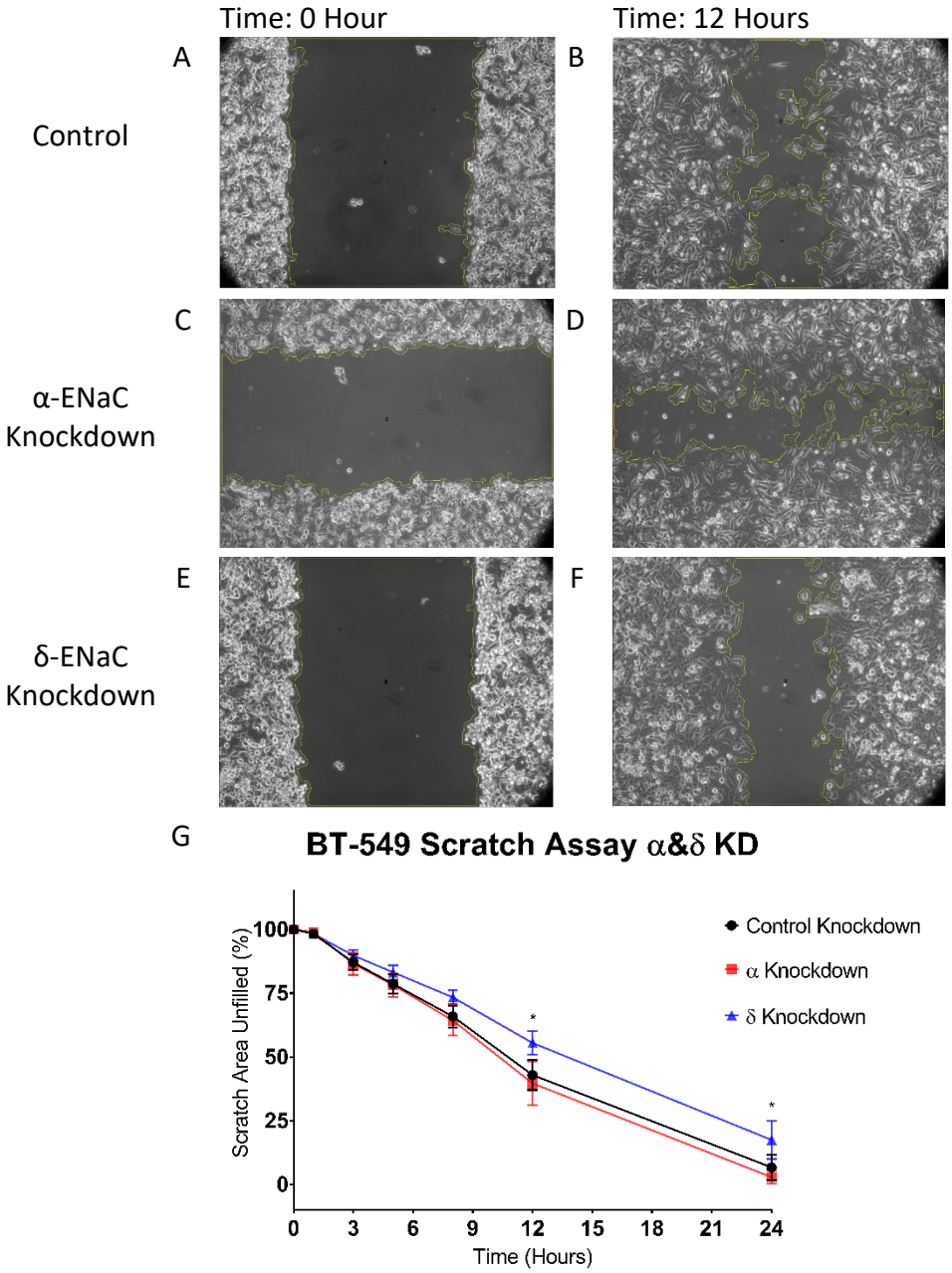

Figure 3.8: The migration of BT-549 cells, in scratch assays, showed no difference when α-ENaC or δ-ENaC was knocked down, compared to the control. A) Control scratch area at time of scratch (0 Hour); B) Control scratch area at 12 hours after the scratch (12 Hours); C) α-ENaC knockdown scratch area at time of scratch; D) α-ENaC knockdown scratch area at 12 hours after the scratch; E) δ-ENaC knockdown scratch area at time of scratch; F) δ-ENaC knockdown scratch area at 12 hours after scratch; G) Pooled results comparing the migratory ability of BT-549 cells with α-ENaC knockdown and δ-ENaC knockdown to control. Mean ±SEM. Analysed using a two-way ANOVA with Tukey's post hoc test. No statistically significant differences were observed between α-ENaC knockdown and control or δ-ENaC knockdown and control. N=4, n=4. *: Significant difference between cell migration of α-ENaC knockdown and δ-ENaC knockdown ($P<0.05$).

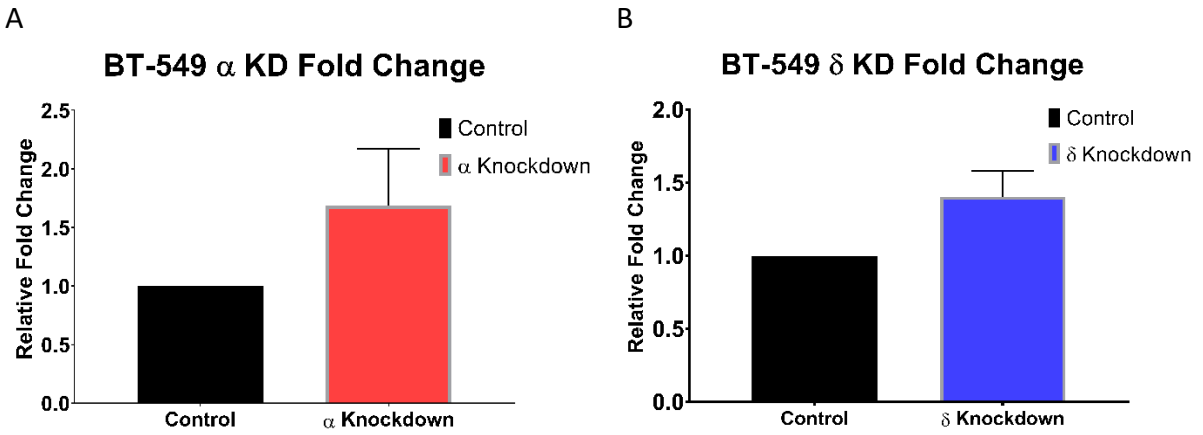

Figure 3.9: Knockdown of α-ENaC or δ-ENaC in BT-549 cells. A) α-ENaC knockdown had an approximately 1.7-fold mean increase in α-ENaC mRNA relative to the control. Mean ±SEM. This was not a statistically significant difference when analysed using an unpaired t-test with Welch's correction. P=0.2954, N=3, n=3. B) δ-ENaC knockdown had an approximately 1.4-fold mean increase in δ-ENaC mRNA relative to the control. This was not statistically significant when analysed using an unpaired t-test with Welch's correction. P=0.1478, N=3, n=3.

3.3 Aldosterone and α-ENaC Overexpression

This project aimed to build upon the results of a previous honours student's project which also investigated the role of ENaC in breast cancer cell migration (McQueen, 2018). In the previous project, pharmacological agents: amiloride and aldosterone were used. Amiloride was used to inhibit ENaC activity, with concentrations of 2nM and 10nM. Aldosterone was used to increase ENaC expression using concentrations of 5nM and 10nM. The use of 10nM of aldosterone was observed to significantly increase migration in BT-549 cells but significantly reduce migration in MDA-MB-231 cells. The results of the project described in this thesis observed no effect on cell migration with either overexpression or knockdown of α-ENaC or δ-ENaC in the two mesenchymal breast cancer cell lines utilised. Therefore a 10nM aldosterone scratch assay was performed alongside an α-ENaC overexpression scratch assay to act as a positive control.

3.3.1 MDA-MB-231 Aldosterone and α-ENaC Overexpression

To compare the effect of aldosterone (10nM) and α-ENaC overexpression on breast cancer cell migration, scratch assays were performed utilising MDA-MB-231 cells. At 12 hours post-scratch, the mean percentage of the scratch area unfilled for the control was 44.7%, 38.5% for α-ENaC overexpression, and 39.8% for aldosterone (10nM) (**Figure 3.10B, D, F**). A two-way ANOVA with Tukey's post hoc test was performed and reported no statistically significant differences at any time points between α-ENaC overexpression and control or aldosterone (10nM) and control (N=6; n=6) (**Figure 3.10G**). The results observed in the previous honours project could not be replicated.

3.3.2 BT-549 Cells Aldosterone and α-ENaC Overexpression

These experiments were performed in another mesenchymal breast cancer cell line, BT-549 cells, to compare with the results observed in MDA-MB-231 cells. At 12 hours post-scratch,

the mean percentage of the scratch area unfilled for the control was 69.2%, 63.6% for α-ENaC overexpression and 69.9% for aldosterone (10nM) (**Figure 3.11B, D, F**). A two-way ANOVA with Tukey's post hoc test was performed and reported no statistically significant differences at any time points between α-ENaC overexpression and control or δ-ENaC overexpression and control (N=5; n=5) (**Figure 3.11G**). The results observed in the previous honours project could not be replicated.

Due to time constraints, qPCR was not performed. As α-ENaC overexpression was successful in previous experiments utilising the same protocol, it was assumed that overexpression was successful in these experiments. The functional status of the aldosterone used in these experiment was tested after obtaining the results, to determine whether it was able to increase ENaC activity. An Ussing chamber current measurement experiment was performed and the aldosterone used in this experiment was not able to increase ENaC current compared to the control, as previously observed when treating with aldosterone. This suggests that this particular tube of aldosterone was non-functional (Cheung, data not shown).

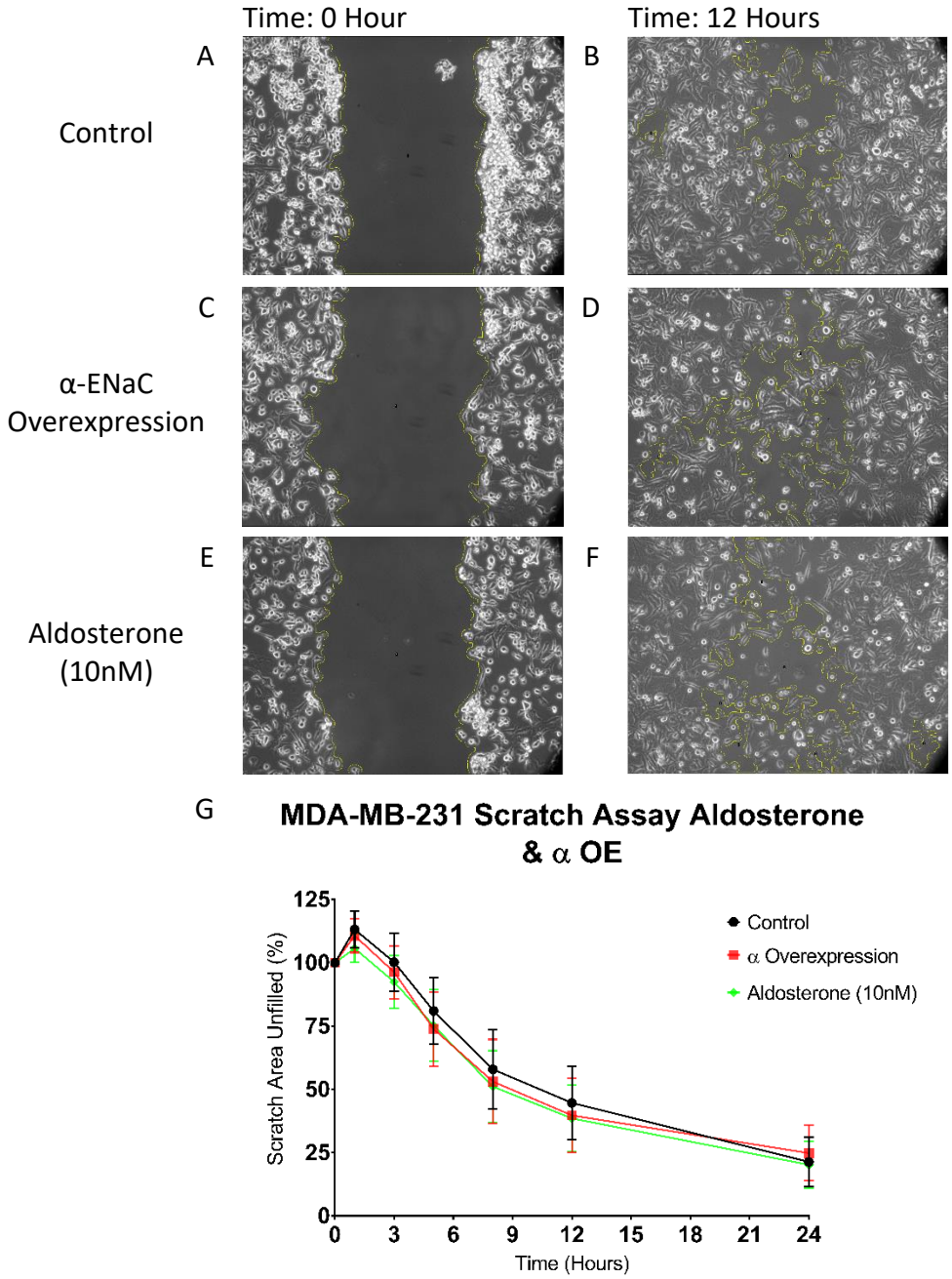

Figure 3.10: The migration of MDA-MB-231 cells, in scratch assays, showed no difference with α-ENaC overexpression or 10nM aldosterone, compared to the control. A) Control scratch area at time of scratch (0 Hour); B) Control scratch area at 12 hours after the scratch (12 Hours); C) α-ENaC overexpression scratch area at time of scratch (0 Hour); D) α-ENaC overexpression scratch area at 12 hours after the scratch (12 Hours); E) Aldosterone (10nM) scratch area at time of scratch (0 Hour); F) Aldosterone (10nM) scratch area at 12 hours after scratch (12 Hours); G) Pooled results comparing the migratory ability of MDA-MB-231 cells with α-ENaC overexpression and Aldosterone (10nM) to control. Mean ±SEM. Analysed using a two-way ANOVA with Tukey's post hoc test. No statistically significant differences were

observed between α-ENaC overexpression and control or aldosterone (10nM) and control. N=6, n=6.

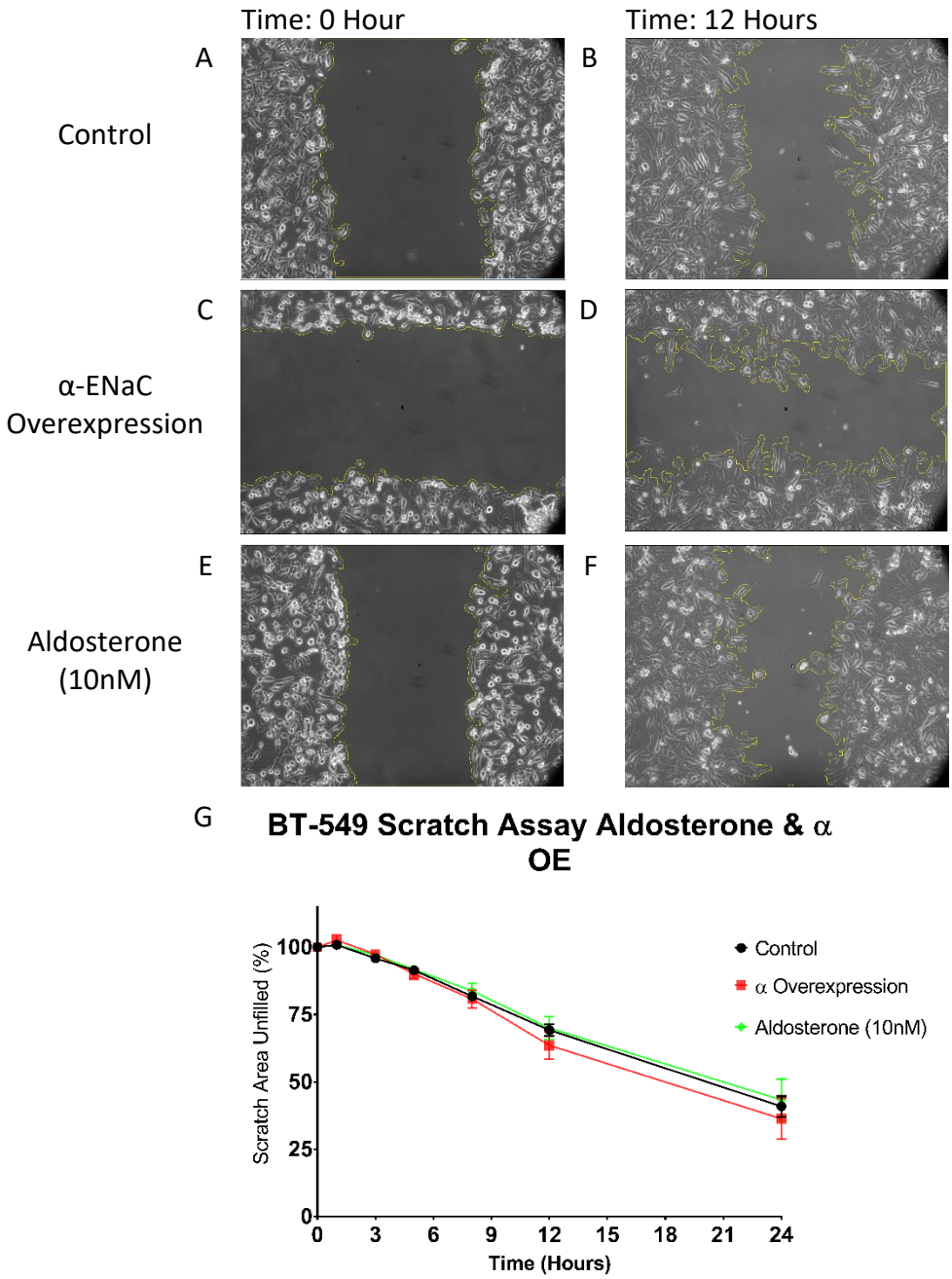

Figure 3.11: The migration of BT-549 cells, in scratch assays, showed no difference with α-ENaC overexpression or 10nM aldosterone, compared to the control. A) Control scratch area at time of scratch (0 Hour); B) Control scratch area at 12 hours after the scratch (12 Hours); C) α-ENaC overexpression scratch area at time of scratch (0 Hour); D) α-ENaC overexpression scratch area at 12 hours after the scratch (12 Hours); E) Aldosterone (10nM) scratch area at time of scratch (0 Hour); F) Aldosterone (10nM) scratch area at 12 hours after scratch (12 Hours); G) Pooled results comparing the migratory ability of BT-549 cells with α-ENaC overexpression and Aldosterone (10nM) to control. Mean ±SEM. Analysed using a two-way ANOVA with Tukey's post hoc test. No statistically significant differences were observed between α-ENaC overexpression and control or aldosterone (10nM) and control. N=5, n=5.

4 Discussion

ENaC is a sodium ion channel that is found in many epithelia including the kidney, lung, colon, and mammary tissue (Boyd & Náray-Fejes-Tóth, 2007; Hanukoglu & Hanukoglu, 2016). ENaC is a heterotrimer consisting of either α-ENaC or δ-ENaC, β-ENaC, and γ-ENaC and plays an important role in the regulation of blood pressure (Hanukoglu & Hanukoglu, 2016; Noreng *et al.*, 2018).

The role of ENaC in regulating EMT has been suggested with preliminary data from the McDonald laboratory that reported higher mRNA levels of ENaC in epithelial-like breast cancer cell lines than mesenchymal-like breast cancer cell lines. This suggests that altering ENaC mRNA level may lead to cells acquiring different characteristics, such as becoming more migratory, which are important in the progression of cancer into a metastatic disease. ENaC has been previously reported to be involved in cell migration. A role for ENaC in cell migration has been shown in keratinocytes, vascular smooth muscle cells, D54-MG glioblastoma multiforme cells, and in BeWo choriocarcinoma cells (Grifoni *et al.*, 2006; del Mónaco *et al.*, 2009; Kapoor *et al.*, 2009; Yang *et al.*, 2013). These studies show that altering ENaC expression effects cell migration and suggest that overexpressing or knocking down ENaC in breast cancer cells could alter cell migration.

The mRNA levels of ENaC subunits has been correlated with breast cancer prognosis. As seen in (**Figure 1.3**), using a bioinformatics tool developed by Györffy et al, (2010), patients with higher expression of α-ENaC or δ-ENaC were correlated with having a better prognosis when compared to patients with lower expression of α-ENaC or δ-ENaC.

Breast cancer is an important disease worldwide as it is the most common and deadliest form of female cancer. This is reflected in New Zealand with a high age standardised incidence rate of 94.1 cases per 100,000 women in 2017 (Ministry of Health, 2019). An age standardised mortality rate of 17.3 deaths per 100,000 women was reported in 2016, with almost 700 deaths (Ministry of Health, 2018). The majority of breast cancer deaths are due to metastases, therefore finding new treatments, especially those that can target metastatic disease, is an important direction for research. Due to their location on the cell membrane and their role in many cellular functions, ion channels such as ENaC may be an attractive potential target for treatment of diseases including breast cancer.

This project aimed to understand the role of ENaC in breast cancer cell migration and build on the results of a previous honours project that used amiloride and aldosterone to alter ENaC activity and mRNA level. To investigate the role of ENaC in breast cancer cell migration in this project, two ENaC subunits, α-ENaC and δ-ENaC, were either overexpressed or knocked down. Scratch assays were used as a functional test of cell migration and qPCR was performed to confirm whether transfection resulted in a change in ENaC mRNA level. It was hypothesised that overexpression of α-ENaC or δ-ENaC will cause an increase in migration of mesenchymal breast cancer cells and knockdown of α-ENaC or δ-ENaC will cause a decrease in migration of mesenchymal breast cancer cells.

4.1 The Effect of Overexpressing of α-ENaC or δ-ENaC in Scratch Assays

Overexpression of α-ENaC or δ-ENaC was performed in two triple negative, mesenchymal breast cancer cell lines, MDA-MB-231 and BT-549. Cell migration was assessed using scratch assays with photographs taken at multiple time points. Area of the scratch was calculated as

a percentage of the original scratch area at time 0. In MDA-MB-231 cells, overexpression of α-ENaC or δ-ENaC did not have an effect on migration compared to the control. In BT-549 cells, overexpression of α-ENaC or δ-ENaC did not have an effect on migration compared to the control. This contradicted my hypothesis that overexpression of α-ENaC or δ-ENaC in mesenchymal breast cancer cell lines would lead to an increase in breast cancer cell migration. This was not a result of unsuccessful transfection as qPCR showed a statistically significant increases in both α-ENaC and δ-ENaC mRNA in BT-549 cells and a statistically significant increase of δ-ENaC mRNA in MDA-MB-231 cells. α-ENaC overexpression was trending towards statistical significance with a P value of 0.09, which is likely due to the varying magnitude of the increase.

4.2 The Effect of Knockdown of α-ENaC or δ-ENaC in Scratch Assays

Knockdown of α-ENaC or δ-ENaC was also performed in two triple negative, mesenchymal breast cancer cell lines, MDA-MB-231 and BT-549. This was performed to observe whether reducing ENaC expression would result in a change in breast cancer cell migration and was compared with the overexpression results. In MDA-MB-231 cells, knockdown of α-ENaC or δ-ENaC did not have an effect on migration, when compared to control. Furthermore, knockdown of α-ENaC or δ-ENaC in BT-549 cells did not have an effect on migration, compared to the control. This contradicted my hypothesis that knockdown of α-ENaC or δ-ENaC in mesenchymal breast cancer cell lines would lead to a decrease in breast cancer cell migration. These results are likely due to unsuccessful transfection as no statistically significant difference in mRNA levels were observed in the qPCR experiments of both cell lines between the α-ENaC knockdown and control, or the δ-ENaC knockdown and control. Interestingly there was a

statistically significant difference in migration between α-ENaC knocked down cells and δ-ENaC knocked down cells in BT-549 cells. This suggests that δ-ENaC is more involved in breast cancer cell migration than α-ENaC. However, this could be due to biological variability as qPCR experiments showed unsuccessful knockdown of both α-ENaC and δ-ENaC.

4.3 Aldosterone Scratch Assays

This project was based on the results of a previous project that also investigated the role of ENaC in breast cancer cell migration (McQueen, 2018). In the previous project, pharmacological agents were utilised with amiloride used to inhibit ENaC and aldosterone to increase ENaC expression. Statistically significant differences in migration were reported when they were used with MDA-MB-231 and BT-549 cells in scratch assays. With 10nM of aldosterone, MDA-MB-231 cells saw a statistically significant reduction in migration at 12 hours after scratch when compared to control. In BT-549 cells treated with 10nM of aldosterone, a statistically significant increase in migration was observed at 12 hours after scratch, when compared to control. As the overexpression and knockdown of α-ENaC or δ-ENaC showed no significant difference compared to the control, there was an attempt to reproduce the previously reported 10nM aldosterone results as a positive control, and was performed alongside α-ENaC overexpression and control. The results of the previous project could not be replicated in these experiments. In MDA-MB-231 cells, no statistically significant differences were observed between either the α-ENaC overexpression and the control or 10nM of aldosterone and the control. The same result was seen in BT-549 cells as there was no statistically significant difference was observed between α-ENaC or 10nM aldosterone and control. As qPCR had not been performed due to time constraints, it is not known whether the

α-ENaC overexpression result was due to unsuccessful transfection. As previous experiments have shown successful α-ENaC overexpression using the same transfection protocol, it was assumed that it was successful in these experiments. The status of the aldosterone used in these experiment was tested after obtaining the results to determine whether it was able to increase ENaC activity. An Ussing chamber current measurement experiment was performed using mouse cortical collecting duct (mCCD) epithelial cells. These cells were incubated with either aldosterone or vehicle followed by ENaC current measurements. The aldosterone used in this experiment was not able to increase ENaC current compared to the control. Previously, this protocol showed a significant increase in ENaC current with aldosterone therefore suggesting that this particular tube of aldosterone was non-functional (Cheung, data not shown). This provides an explanation for why the aldosterone cell migration results of the previous project could not be replicated.

4.4 Possible Explanations for the Lack of Effect of Changing ENaC mRNA levels on Cell Migration

Possible explanations for why altering α-ENaC or δ-ENaC mRNA levels had no effect on breast cancer cell migration could be due to: 1) other targets of aldosterone, 2) the breast cancer cell lines used in this project were in a more proliferative transition state rather than migratory, and 3) the need for the other ENaC subunits.

This project was based on results of a previous honours project that also investigated the role of ENaC in breast cancer cell migration. Results from that project showed that aldosterone was able to alter the migration of breast cancer cell line cells compared to a control (McQueen, 2018). This project aimed to build on those results by specifically targeting α-ENaC and δ-ENaC

subunits. The results from this project however, suggest that altering mRNA levels of α-ENaC or δ-ENaC has no effect on breast cancer cell migration, therefore, other targets of aldosterone may be responsible for the previously observed changes in cell migration.

Aldosterone has been shown to be involved in breast cancer cell migration mediated by the G-Protein estrogen receptor (GPER) (Rigiracciolo *et al.*, 2016). Aldosterone is a mineralocorticoid hormone produced within the adrenal gland (Booth *et al.*, 2002). It has a well characterised role in responding to low blood pressure conditions as part of the RAAS pathway (Booth *et al.*, 2002). Within breast cancer cells, aldosterone binds to the MR which can interact with GPER, and mediate the interaction of GPER and epidermal growth factor receptor (EGFR) to initiate EGFR/extracellular signal-regulated kinases (ERK) signalling. This can result in the upregulation of the sodium hydrogen exchanger 1 (NHE1) (Rigiracciolo *et al.*, 2016). NHE1 is an exchanger that transports one sodium ion into the cell for one proton out of the cell, and has a role in pH regulation, sodium transport, cell volume regulation, and cell migration (Stock & Schwab, 2006; Parker *et al.*, 2015). Involvement of NHE1 in breast cancer cell migration mediated by aldosterone has been demonstrated in SkBr3 breast cancer cells. SkBr3 cells had MR knocked down or transfected with control siRNA and were exposed to 10pM of aldosterone or vehicle for 48 hours. Scratch assays were then performed to compare cell migration. SkBr3 cells with MR knocked down were not able to migrate in response to aldosterone. NHE1 was shown to be important in this process as inhibition of NHE1 with cariporide showed a similar inability to migrate in response to aldosterone. This suggest that an upregulation of NHE1 by aldosterone rather than of ENaC could be responsible for the increase in cell migration observed in the previous honours project.

Unpublished data from the McDonald Laboratory suggests that ENaC is involved in breast cancer cell proliferation. Using EdU cell proliferation assays, overexpression of α-ENaC was able to reduce the percentage of proliferating cells in the same breast cancer cell lines used in this project: MDA-MB-231 and BT-549. When α-ENaC was knocked down in these cell lines, an increase in the percentage of proliferating cells was observed. Using the same overexpression and knockdown transfection protocol used to study proliferation, the results of my project suggest that ENaC, specifically α-ENaC and δ-ENaC, have no role in breast cancer cell migration. While cell migration and proliferation are often linked, some studies show they can be independent of each other. Feng et al (2017), showed that while gonadotropin exposure was able to significantly increase migration of SKOV3 and HO8910 ovarian cancer cells, it did not increase cellular proliferation (Feng *et al.*, 2017). Another study by Zhou et al (2017), showed that silencing Serpin Peptidase Inhibitor, clade A member 3 (SERPINA3) with siRNA led to a significant decrease in migration but with no change in proliferation of MMRU melanoma cells (Zhou *et al.*, 2017).

A review of EMT in cancer progression has stated that there are different hybrid states between the epithelial and mesenchymal states (Pastushenko & Blanpain, 2019). Cells in these hybrid states express markers of both epithelial and mesenchymal phenotypes. This can be seen with changes in the two isoforms of transcription factor Paried related homeobox 1 (Prrx1). Overexpression of Prrx1a leads to a transition state that is closer to an epithelial phenotype, with higher E-cadherin levels and decreased invasion, and is associated with metastatic outgrowth in new tissue. Overexpression of Prrx1b leads to a transition state that is closer to a mesenchymal phenotype, with decreased E-cadherin levels and increased

invasiveness, and is associated with increased dissemination of tumour cells (Takano *et al.*, 2016). Another study demonstrated the existence of these hybrid transition states and their different functional capabilities (Pastushenko *et al.*, 2018). Six subsets of hybrid phenotypes were identified when using a genetic mouse model of skin squamous cell carcinoma. These subsets were characterised based on the expression of three markers that were most frequently heterogeneously expressed during EMT: CD106, CD51, and CD61. These subsets displayed different functional characteristics with different subtypes becoming more invasive or more metastatic than others (Pastushenko *et al.*, 2018). Hybrid transition states are also seen within breast cancer cells (Yu *et al.*, 2013). Breast cancer tissue cells were analysed based the expression of several epithelial and mesenchymal markers. Many cells were observed to co-express markers of both epithelial and mesenchymal phenotypes with the proportion of cells expressing either an epithelial, mesenchymal, or hybrid phenotype able to change with response to treatment and disease progression (Yu *et al.*, 2013). This demonstrates the existence of hybrid transition states and that these hybrid transition states may be functionally different from one another. This means that one transition state could have a migratory phenotype while another could be more proliferative (**Figure 4.1**). If the cell lines used in this project, MDA-MB-231 and BT-549, were derived from cells in a more proliferative hybrid state, this could explain why no change in cell migration was observed in this project.

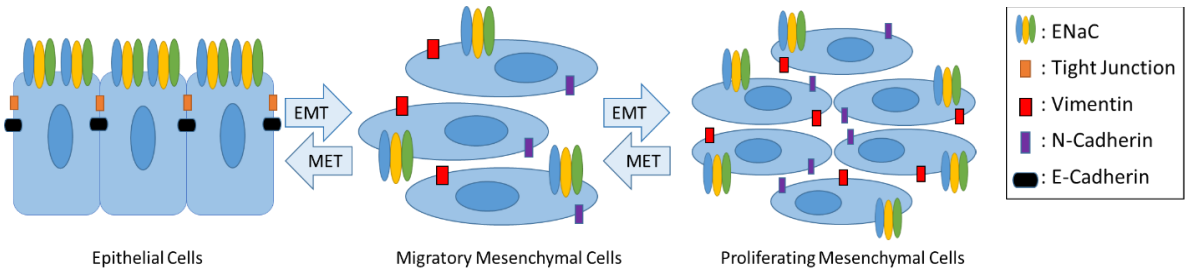

Figure 4.1: Proposed mechanism of Epithelial to Mesenchymal Transition with functionally different hybrid transition states. Presents cells in an epithelial state or in two separate hybrid transition states: a migratory transition state and a proliferating transition state.

ENaC is a heterotrimer consisting of an α-ENaC or δ-ENaC subunit, a β-ENaC subunit, and a γ-ENaC subunit. Individual α-ENaC or δ-ENaC subunits are sufficient to produce an amiloride sensitive current, however when co-expressed with β-ENaC and γ-ENaC the amiloride sensitive current increased markedly (Canessa *et al.*, 1994; McDonald *et al.*, 1995; Waldmann *et al.*, 1995). In this project, changes in cell migration were only investigated with changes in expression of either α-ENaC or δ-ENaC subunits. However, before the initiation of this project, unpublished proliferation data from the McDonald laboratory suggested that there was no difference between α-ENaC and αβγ-ENaC on the effect on proliferation. Therefore, the use of single subunits of ENaC was thought to be sufficient to understand their role in breast cancer cell migration. The unpublished proliferation data also demonstrated that inhibition of ENaC produced a similar increase in the percentage of proliferating cells to the knockdown of ENaC subunits. This suggested that ENaC activity was important, and so α-ENaC or δ-ENaC, the two subunits that are sufficient to produce an amiloride sensitive current, were selected for this project. Cell migration may however be different to cell proliferation, so altering the expression of β-ENaC and γ-ENaC subunit in tandem with α-ENaC or δ-ENaC may help delineate the true role of ENaC in breast cancer cell migration.

4.5 Limitations and Next Steps

4.5.1 Cell Passage Effects

The passage number of the cells used in this project was at approximately passage number 60 when scratch assay experiments began. Cell passage effects can alter transfection efficiency, protein expression, and diverge cells away from the original tissue from which it was derived (Mouriaux *et al.*, 2016; American Type Culture Collection, 2019). In this project qPCR was used to validate the transfection of the cells. This works by comparing the level of mRNA within the cells and inferring a change in protein levels. Due to the use of high passage number cells, this may not be the case and so no functional changes would be observed (American Type Culture Collection, 2019). Follow up experiments should be performed with low passage number cells and include western blotting to validate a change in protein levels.

4.5.2 Knockdown of α-ENaC and δ-ENaC

The knockdown of α-ENaC or δ-ENaC was attempted using siRNA to observe what effect this may have on breast cancer cell migration. The results from the scratch assays performed in this project showed that knockdown of α-ENaC or δ-ENaC had no effect on cell migration compared to the control in MDA-MB-231 and BT-549 mesenchymal breast cancer cells. This however could be due to unsuccessful transfection or non-functional siRNA as results from the qPCR experiments showed no significant difference in mRNA level of either α-ENaC or δ-ENaC when compared to the control. The knockdown experiments should be repeated using new components to elucidate the true effect that knockdown of α-ENaC or δ-ENaC has on breast cancer cell migration.

4.5.3 Positive Controls

To ensure the scratch assays are functioning correctly, positive controls should be utilised. Other publications have used a variety of positive controls including 10% FBS, if serum free media is used, and Allantoin (Bullard *et al.*, 2018; Muniandy *et al.*, 2018). Phalliodin conjugated with a fluorescent marker could be used as a pseudo marker for cell migration. This would allow for the visualisation of the F-actin cytoskeleton to determine whether it displays morphological features that would be expected within migrating cells such as lamellipodium protrusions (Schwab, 2001). Functional assays such as Ussing chamber current measurements could not be performed with these cells as do not form an epithelium. Follow up projects should be performed with a positive control.

4.5.4 Serum Media

The scratch assays were performed in media containing 10% FBS to match the conditions used by the previous honours project. This decision was made as the cells used were not reaching confluence in serum free media. It is unlikely however, that proliferation had a large effect in reducing the size of the scratch area as the doubling time of the breast cancer cell lines used in this project was reported in publications as at least 25 hours (Fonagy *et al.*, 1994; Limame *et al.*, 2012). Follow up projects using scratch assays could use serum free media to arrest the cell cycle or add inhibitors of proliferation such as Mitomycin C and Cytosine β-d-arabinofuranoside hydrochloride to remove any effect of proliferation (Giretti *et al.*, 2014; Vang Mouritzen & Jenssen, 2018). Monitoring levels of proliferation markers such as Ki-67 may also be useful to determine whether there is any contribution of proliferation to the results (Shi *et al.*, 2019). These will ensure that the results of the scratch assay are solely due to cell migration.

4.5.5 Technical Difficulties with qPCR and Scratch Assays

Due to the high sensitivity of qPCR, special care had to be taken when performing these experiments. Contamination of primers and other components early in the project meant that validation of overexpression and knockdown experiments was delayed. New components had to be ordered and these were aliquoted to reduce further contamination. A specific area and lab coat was used for qPCR with ethanol sprayed on all surfaces to reduce contamination. Loading of the qPCR plate was completed on ice to ensure the cDNA was not degraded. When loading cDNA into the wells, special care was taken to ensure the pipette tip was not carried over wells which did not contain the same cDNA to avoid contamination.

Keeping the size of the scratch area consistent was another task that required special care. Although these results were normalised by taking a percentage of the original scratch area, comparing a large initial scratch area with a smaller initial scratch area would confound the results. Another way of analysing the data could be to calculate the rate of cell migration with live-cell microscopy, which could reduce the confounding effect of the initial size of the scratch area (Jonkman *et al.*, 2014; Bobadilla *et al.*, 2019).

4.5.6 Alternative Cell Migration Assays

Only one migration assay, the scratch assay, was used in this project. Employing the use of another migration assay could either corroborate or contradict the results in this project. Cell exclusion zone assays are another migration assay which use similar rationale to the scratch assays. This assay uses a cell seeding stopper to occlude a region on the plate from cell growth. The cells can be seeded around the stopper, and when confluence is reached, the stopper can be removed to begin the experiment (Hulkower & Herber, 2011). This has some advantages over the scratch assays used in this project as no cells are damaged to produce the area that

is uncovered by cells and the size of the uncovered area is less variable compared to the scratch assays (Hulkower & Herber, 2011).

Boyden chamber assays are also another migration assay that could be used (Justus *et al.*, 2014). This assay uses transwells with an insert with a porous filter membrane. Serum free media is added to the insert and serum containing media is added to the bottom well. This provides a chemotactic gradient for cells to migrate towards. Cells are seeded onto the insert and can migrate through the porous filter membrane, toward the chemo-attractant. The amount of cells able to migrate into the bottom well can be quantified and compared with different experimental conditions. This can also be used as an invasion assay with Matrigel simulating the extracellular matrix. A layer of Matrigel is added over the filter membrane before the cells are seeded. The amount of cells able to reach the bottom well can be quantified and represents the invasive capability of the cells (Justus *et al.*, 2014).

4.5.7 Future Directions

Due to time constraints the effect of overexpressing or knocking down α-ENaC and δ-ENaC on EMT marker expression could not be explored. As ENaC has been shown to be differentially expressed within epithelial and mesenchymal breast cancer cell lines, investigating whether overexpression or knockdown of ENaC could possible induce EMT or MET would be an interesting direction of research. This can be explored by performing qPCR with primers for E-cadherin, an epithelial marker, and Vimentin and N-cadherin, two mesenchymal markers.

As knockdown of α-ENaC and δ-ENaC was not successful in this project, producing cell lines with a stable knockdown of α-ENaC and δ-ENaC subunits may be another option. This can be

achieved using viral vectors and shRNA. The shRNA can be integrated into the DNA, and induce stable knockdown through RNA interference activity (Moore *et al.*, 2010).

While ENaC may not have a role in breast cancer cell migration, it may still be involved in other aspects of breast cancer, such as cellular invasion. Alterations to cellular invasion with changes to ENaC can be investigated using the Boyden chamber assay described in Section 4.5.6.

Investigating whether ENaC is involved in cell morphology may be another aspect that could be investigated. A study by Yang et al, observed that co-culturing breast cancer MCF-7 and MDA-MB-231 cells with different subsets of macrophages led to changes in cellular morphology (Yang *et al.*, 2016). A ratio of mid-point diameter and cell perimeter was used as a way to quantify cell morphology with a higher ratio associated with an epithelial phenotype while a lower ratio with a mesenchymal phenotype. They found that co-culturing MCF-7 epithelial breast cancer cells with M2 macrophages promoted a mesenchymal phenotype as the mid-point diameter-cell perimeter ratio decreased compared to control and co-culturing with M0 or M1 macrophages (Yang *et al.*, 2016). A similar effect was seen in MDA-MB-231 mesenchymal breast cancer cells as co-culturing with M2 macrophages decreased the mid-point diameter-cell perimeter ratio while co-culturing with M1 macrophages increased the ratio, compared to control and co-culturing with M0 macrophages (Yang *et al.*, 2016). This suggested that M1 macrophages promote an epithelial phenotype while M2 macrophages promote a mesenchymal phenotype (Yang *et al.*, 2016). Investigating whether altering ENaC could alter cell morphology in a similar way could be a possible direction of further research.

5 Conclusion

The aim of this project was to investigate whether ENaC has a role in breast cancer cell migration. To do this the expression of two ENaC subunits, α-ENaC and δ-ENaC, were overexpressed in two mesenchymal breast cancer cell lines. It was hypothesised that overexpression of α-ENaC or δ-ENaC will cause an increase in the migration of mesenchymal breast cancer cells. The results of this project contradict the hypotheses as no significant difference in cell migration was observed when α-ENaC or δ-ENaC was overexpressed in two mesenchymal breast cancer cell lines. As knockdown of α-ENaC and δ-ENaC was not successful, the hypothesis that knockdown of α-ENaC of δ-ENaC will cause a decrease in the migration of mesenchymal breast cancer cells could not be confirmed or denied. This project did have its limitations and follow up experiments should be performed with these being addressed to observe whether there is a change in breast cancer cell migration. ENaC has been shown to be involved in proliferation of breast cancer cells and so could also be involved in other aspects of breast cancer metastases. Investigating a possible role of ENaC in invasion and cellular morphology regulation of breast cancer cells are possible directions for future research.

Reference List

Amara S, Ivy MT, Myles EL & Tiriveedhi V. (2016). Sodium Channel γENaC Mediates Il-17 Synergized High Salt Induced Inflammatory Stress in Breast Cancer Cells. *Cellular Immunology* **302,** 1-10.

American Type Culture Collection. (2019). Passage Number Effects in Cell Lines. Available at: https://www.atcc.org/~/media/PDFs/Technical%20Bulletins/tb07.ashx [Accessed: 4/10/19]

Bobadilla AVP, Arévalo J, Sarró E, Byrne HM, Maini PK, Carraro T, Balocco S, Meseguer A & Alarcón T. (2019). In Vitro Cell Migration Quantification Method for Scratch Assays. *Journal of The Royal Society Interface* **16,** 20180709.

Booth RE, Johnson JP & Stockand JD. (2002). Aldosterone. *Advances in Physiology Education* **26,** 8-20.

Boyd C & Náray-Fejes-Tóth A. (2007). Steroid-Mediated Regulation of the Epithelial Sodium Channel Subunits in Mammary Epithelial Cells. *Endocrinology* **148,** 3958-3967.

Bray F, Ferlay J, Soerjomataram I, Siegel RL, Torre LA & Jemal A. (2018). Global Cancer Statistics 2018: Globocan Estimates of Incidence and Mortality Worldwide for 36 Cancers in 185 Countries. *CA: A Cancer Journal for Clinicians* **68,** 394-424.

Breast Cancer Foundation NZ. (2019). Breast Cancer Treatment Options. Available at: https://www.breastcancerfoundation.org.nz/breast-cancer/treatment-options, [Accessed: 20/05/19]

Bullard J, Lei J, Lim J, Massee M, Fallon A & Koob T. (2018). Evaluation of Dehydrated Human Umbilical Cord Biological Properties for Wound Care and Soft Tissue Healing: Properties of Dehydrated Human Umbilical Cord for Wound Care. *Journal of Biomedical Materials Research Part B: Applied Biomaterials* **107,** 1035-1046.

Campbell K. (2018). Contribution of Epithelial-Mesenchymal Transitions to Organogenesis and Cancer Metastasis. *Current Opinion in Cell Biology* **55,** 30-35.

Canessa CM, Schild L, Buell G, Thorens B, Gautschi I, Horisberger J-D & Rossier BC. (1994). Amiloride-Sensitive Epithelial Na+ Channel Is Made of Three Homologous Subunits. *Nature* **367,** 463-467.

Chang SS, Grunder S, Hanukoglu A, Rösler A, Mathew PM, Hanukoglu I, Schild L, Lu Y, Shimkets RA, Nelson-Williams C, Rossier BC & Lifton RP. (1996). Mutations in Subunits of the Epithelial Sodium Channel Cause Salt Wasting with Hyperkalaemic Acidosis, Pseudohypoaldosteronism Type 1. *Nature Genetics* **12,** 248-253.

Chen S & Parmigiani G. (2007). Meta-Analysis of BRCA1 and BRCA2 Penetrance. *Journal of Clinical Oncology* **25,** 1329-1333.

Davies EL. (2016). Breast Cancer. *Medicine* **44,** 42-46.

Davis FM, Azimi I, Faville RA, Peters AA, Jalink K, Putney JW, Jr., Goodhill GJ, Thompson EW, Roberts-Thomson SJ & Monteith GR. (2014). Induction of Epithelial-Mesenchymal Transition (EMT) in Breast Cancer Cells Is Calcium Signal Dependent. *Oncogene* **33,** 2307-2316.

del Mónaco SM, Marino GI, Assef YA, Damiano AE & Kotsias BA. (2009). Cell Migration in BeWo Cells and the Role of Epithelial Sodium Channels. *Journal of Membrane Biology* **232,** 1-13.

Elston CW & Ellis IO. (1991). Pathological Prognostic Factors in Breast Cancer. I. The Value of Histological Grade in Breast Cancer: Experience from a Large Study with Long-Term Follow-Up. *Histopathology* **19,** 403-410.

Feng D, Zhao T, Yan K, Liang H, Liang J, Zhou Y, Zhao W & Ling B. (2017). Gonadotropins Promote Human Ovarian Cancer Cell Migration and Invasion Via a Cyclooxygenase 2-Dependent Pathway. *Oncology Reports* **38,** 1091-1098.

Fonagy A, Swiderski C, Ostrovsky AM, Bolton WE & Freeman JW. (1994). Effect of Nucleolar P120 Expression Level on the Proliferation Capacity of Breast Cancer Cells. *Cancer Research* **54,** 1859.

Fortunato A. (2017). The Role of hERG1 Ion Channels in Epithelial-Mesenchymal Transition and the Capacity of Riluzole to Reduce Cisplatin Resistance in Colorectal Cancer Cells. *Cellular Oncology* **40,** 367-378.

Garg M. (2013). Epithelial-Mesenchymal Transition - Activating Transcription Factors - Multifunctional Regulators in Cancer. *World Journal of Stem Cells* **5,** 188-195.

Giraldez T, Rojas P, Jou J, Flores C & Rosa DAdl. (2012). The Epithelial Sodium Channel δ-Subunit: New Notes for an Old Song. *American Journal of Physiology-Renal Physiology* **303,** F328-F338.

Giretti MS, Montt Guevara MM, Cecchi E, Mannella P, Palla G, Spina S, Bernacchi G, Di Bello S, Genazzani AR, Genazzani AD & Simoncini T. (2014). Effects of Estetrol on Migration and Invasion in T47-D Breast Cancer Cells through the Actin Cytoskeleton. *Frontiers in Endocrinology* **5,** 80-80.

Giuliano AE, Connolly JL, Edge SB, Mittendorf EA, Rugo HS, Solin LJ, Weaver DL, Winchester DJ & Hortobagyi GN. (2017). Breast Cancer—Major Changes in the American Joint Committee on Cancer Eighth Edition Cancer Staging Manual. *CA: A Cancer Journal for Clinicians* **67,** 290-303.

Goldhirsch A, Wood WC, Coates AS, Gelber RD, Thürlimann B, Senn HJ & Panel m. (2011). Strategies for Subtypes-Dealing with the Diversity of Breast Cancer: Highlights of the St. Gallen International Expert Consensus on the Primary Therapy of Early Breast Cancer 2011. *Annals of Oncology* **22,** 1736-1747.

Grifoni SC, Gannon KP, Stec DE & Drummond HA. (2006). ENaC Proteins Contribute to VSMC Migration. *American Journal of Physiology-Heart and Circulatory Physiology* **291,** H3076-H3086.

Győrffy B, Lanczky A, Eklund AC, Denkert C, Budczies J, Li Q & Szallasi Z. (2010). An Online Survival Analysis Tool to Rapidly Assess the Effect of 22,277 Genes on Breast Cancer Prognosis Using Microarray Data of 1,809 Patients. *Breast Cancer Research and Treatment* **123,** 725-731.

Hanukoglu I & Hanukoglu A. (2016). Epithelial Sodium Channel (ENaC) Family: Phylogeny, Structure–Function, Tissue Distribution, and Associated Inherited Diseases. *Gene* **579,** 95-132.

Harbeck N & Gnant M. (2017). Breast Cancer. *The Lancet* **389,** 1134-1150.

Hermidorff MM, de Assis LVM & Isoldi MC. (2017). Genomic and Rapid Effects of Aldosterone: What We Know and Do Not Know Thus Far. *Heart Failure Reviews* **22,** 65-89.

Horn J, Åsvold BO, Opdahl S, Tretli S & Vatten LJ. (2013). Reproductive Factors and the Risk of Breast Cancer in Old Age: A Norwegian Cohort Study. *Breast Cancer Research and Treatment* **139,** 237-243.

Hulkower KI & Herber RL. (2011). Cell Migration and Invasion Assays as Tools for Drug Discovery. *Pharmaceutics* **3,** 107-124.

Ji H-L, Zhao R-Z, Chen Z-X, Shetty S, Idell S & Matalon S. (2012). δ Enac: A Novel Divergent Amiloride-Inhibitable Sodium Channel. *American Journal of Physiology-Lung Cellular and Molecular Physiology* **303,** L1013-L1026.

Jin X & Mu P. (2015). Targeting Breast Cancer Metastasis. *Breast Cancer: Basic and Clinical Research* **9,** 23-34.

Jonkman JEN, Cathcart JA, Xu F, Bartolini ME, Amon JE, Stevens KM & Colarusso P. (2014). An Introduction to the Wound Healing Assay Using Live-Cell Microscopy. *Cell Adhesion & Migration* **8,** 440-451.

Justus CR, Leffler N, Ruiz-Echevarria M & Yang LV. (2014). In Vitro Cell Migration and Invasion Assays. *Journal of Visualized Experiments***,** 51046.

Kapoor N, Bartoszewski R, Qadri YJ, Bebok Z, Bubien JK, Fuller CM & Benos DJ. (2009). Knockdown of ASIC1 and Epithelial Sodium Channel Subunits Inhibits Glioblastoma Whole Cell Current and Cell Migration. *The Journal of Biological Chemistry* **284,** 24526-24541.

Kellenberger S & Schild L. (2002). Epithelial Sodium Channel/Degenerin Family of Ion Channels: A Variety of Functions for a Shared Structure. *Physiological Reviews* **82,** 735-767.

Lawrenson R, Lao C, Campbell I, Harvey V, Seneviratne S, Elwood M, Sarfati D & Kuper-Hommel M. (2018). The Impact of Different Tumour Subtypes on Management and Survival of New Zealand Women with Stage I–Iii Breast Cancer. *The New Zealand Medical Journal* **131,** 51-60.

Li Z & Kang Y. (2016). Emerging Therapeutic Targets in Metastatic Progression: A Focus on Breast Cancer. *Pharmacology and Therapeutics* **161,** 79-96.

Limame R, Wouters A, Pauwels B, Fransen E, Peeters M, Lardon F, De Wever O & Pauwels P. (2012). Comparative Analysis of Dynamic Cell Viability, Migration and Invasion Assessments by Novel Real-Time Technology and Classic Endpoint Assays. *PLOS One* **7,** e46536-e46536.

Loffing J, Zecevic M, Féraille E, Kaissling B, Asher C, Rossier BC, Firestone GL, Pearce D & Verrey F. (2001). Aldosterone Induces Rapid Apical Translocation of ENaC in Early Portion of Renal Collecting System: Possible Role of SGK. *American Journal of Physiology-Renal Physiology* **280,** F675-F682.

Makki J. (2015). Diversity of Breast Carcinoma: Histological Subtypes and Clinical Relevance. *Clinical Medicine Insights Pathology* **8,** 23-31.

Matsen CB & Neumayer LA. (2013). Breast Cancer: A Review for the General Surgeon. *JAMA Surgery* **148,** 971-980.

Mazzochi C, Bubien JK, Smith PR & Benos DJ. (2006). The Carboxyl Terminus of the α-Subunit of the Amiloride-Sensitive Epithelial Sodium Channel Binds to F-Actin. *Journal of Biological Chemistry* **281,** 6528-6538.

McDonald FJ, Price MP, Snyder PM & Welsh MJ. (1995). Cloning and Expression of the Beta- and Gamma-Subunits of the Human Epithelial Sodium Channel. *American Journal of Physiology-Cell Physiology* **268,** C1157-C1163.

McQueen SRA. (2018). *The Impact of Epithelial Sodium Channel on Breast Cancer Cell Migration* (Biomedical Sciences Honours Thesis). University of Otago. Dunedin, New Zealand.

Ministry of Health. (2015). Summary of the Breastscreen Aotearoa Mortality Evaluation 1999–2011. *Ministry of Health*, Wellington, New Zealand. Available at: https://www.nsu.govt.nz/system/files/resources/summary-breastscreen-aotearoa-mortality-evaluation-1999-2011_13p_summary_formatted_final.pdf [Accessed: 11/4/19]

Ministry of Health. (2018). Mortality 2016 Data Tables (Provisional). *Ministry of Health, Wellington*. Available at: https://www.health.govt.nz/publication/mortality-2016-data-tables-provisional [Accessed: 29/4/19]

Ministry of Health. (2019). Selected Cancers 2015, 2016, 2017. *Ministry of Health*, Wellington. Available at: https://www.health.govt.nz/publication/selected-cancers-2015-2016-2017 [Accessed: 16/9/19]

Moore CB, Guthrie EH, Huang MT-H & Taxman DJ. (2010). Short Hairpin RNA (shRNA): Design, Delivery, and Assessment of Gene Knockdown. *Methods in Molecular Biology* **629,** 141-158.

Mouriaux F, Zaniolo K, Bergeron M-A, Weidmann C, De La Fouchardière A, Fournier F, Droit A, Morcos MW, Landreville S & Guérin SL. (2016). Effects of Long-Term Serial Passaging on the Characteristics and Properties of Cell Lines Derived from Uveal Melanoma Primary Tumors. *Investigative Ophthalmology and Visual Science* **57,** 5288-5301.

Muniandy K, Gothai S, Tan WS, Kumar SS, Mohd Esa N, Chandramohan G, Al-Numair KS & Arulselvan P. (2018). In Vitro Wound Healing Potential of Stem Extract of Alternanthera Sessilis. *Evidence-Based Complementary and Alternative Medicine* **2018,** 3142073-3142073.

National Center for Biotechnological Information. (2019). Basic Local Alignment Search Tool. Available at: https://blast.ncbi.nlm.nih.gov/Blast.cgi [Accessed: 16/10/19]

Noreng S, Bharadwaj A, Posert R, Yoshioka C & Baconguis I. (2018). Structure of the Human Epithelial Sodium Channel by Cryo-Electron Microscopy. *eLife* **7,** e39340.

Parker MD, Myers EJ & Schelling JR. (2015). Na+-H+ Exchanger-1 (NHE1) Regulation in Kidney Proximal Tubule. *Cellular and Molecular Life Sciences* **72,** 2061-2074.

Pastushenko I & Blanpain C. (2019). EMT Transition States During Tumor Progression and Metastasis. *Trends in Cell Biology* **29,** 212-226.

Pastushenko I, Brisebarre A, Sifrim A, Fioramonti M, Revenco T, Boumahdi S, Van Keymeulen A, Brown D, Moers V, Lemaire S, De Clercq S, Minguijón E, Balsat C, Sokolow Y, Dubois C, De Cock F, Scozzaro S, Sopena F, Lanas A, D'Haene N, Salmon I, Marine J-C, Voet T, Sotiropoulou PA & Blanpain C. (2018). Identification of the Tumour Transition States Occurring During EMT. *Nature* **556,** 463-468.

Plettenberg S, Weiss EC, Lemor R & Wehner F. (2008). Subunits Alpha, Beta and Gamma of the Epithelial Na+ Channel (ENaC) Are Functionally Related to the Hypertonicity-Induced Cation Channel (HICC) in Rat Hepatocytes. *Pflügers Archiv : European Journal of Physiology* **455,** 1089-1095.

Prevarskaya N, Skryma R & Shuba Y. (2018). Ion Channels in Cancer: Are Cancer Hallmarks Oncochannelopathies? *Physiological Reviews* **98,** 559-621.

Rigiracciolo DC, Scarpelli A, Lappano R, Pisano A, Santolla MF, Avino S, De Marco P, Bussolati B, Maggiolini M & De Francesco EM. (2016). GPER Is Involved in the Stimulatory Effects of Aldosterone in Breast Cancer Cells and Breast Tumor-Derived Endothelial Cells. *Oncotarget* **7,** 94-111.

Rojas K & Stuckey A. (2016). Breast Cancer Epidemiology and Risk Factors. *Clinical Obstetrics and Gynecology* **59,** 651-672.

Schwab A. (2001). Ion Channels and Transporters on the Move. *Physiology* **16,** 29-33.

Seneviratne S, Lawrenson R, Harvey V, Ramsaroop R, Elwood M, Scott N, Sarfati D & Campbell I. (2016). Stage of Breast Cancer at Diagnosis in New Zealand: Impacts of Socio-Demographic Factors, Breast Cancer Screening and Biology. *BMC Cancer* **16,** 129.

Shi Y, Lim SK, Liang Q, Iyer SV, Wang H-Y, Wang Z, Xie X, Sun D, Chen Y-J, Tabar V, Gutin P, Williams N, De Brabander JK & Parada LF. (2019). Gboxin Is an Oxidative Phosphorylation Inhibitor That Targets Glioblastoma. *Nature* **567,** 341-346.

Shimkets RA, Warnock, DG, Bositis, CM, Nelson-Williams, C, Hansson, JH, Schambelan, M, Gill, JR, Jr., Ulick, S, Milora, RV, Findling, JW, Canessa, CM, Rossier, BC, and Lifton, RP. (1994). Liddle's Syndrome: Heritable Human Hypertension Caused by Mutations in the β Subunit of the Epithelial Sodium Channel. *Cell* **79,** 407-414.

Sinn H-P & Kreipe H. (2013). A Brief Overview of the WHO Classification of Breast Tumors, 4th Edition, Focusing on Issues and Updates from the 3rd Edition. *Breast Care* **8,** 149-154.

Stock C & Schwab A. (2006). Role of the Na+/H+ Exchanger NHE1 in Cell Migration. *Acta Physiologica* **187,** 149-157.

Strautnieks SS, Thompson RJ, Gardiner RM & Chung E. (1996). A Novel Spice–Site Mutation in the γ Subunit of the Epithelial Sodium Channel Gene in Three Pseudohypoaldosteronism Type 1 Families. *Nature Genetics* **13,** 248-250.

Sun YS, Zhao Z, Yang ZN, Xu F, Lu HJ, Zhu ZY, Shi W, Jiang J, Yao PP & Zhu HP. (2017). Risk Factors and Preventions of Breast Cancer. *International Journal of Biological Sciences* **13,** 1387-1397.

Swick AG, Janicot M, Cheneval-Kastelic T, McLenithan JC & Lane MD. (1992). Promoter-cDNA-Directed Heterologous Protein Expression in Xenopus Laevis Oocytes. *Proceedings of the National Academy of Sciences of the United States of America* **89,** 1812.

Takano S, Reichert M, Bakir B, Das KK, Nishida T, Miyazaki M, Heeg S, Collins MA, Marchand B, Hicks PD, Maitra A & Rustgi AK. (2016). Prrx1 Isoform Switching Regulates Pancreatic Cancer Invasion and Metastatic Colonization. *Genes and Development* **30,** 233-247.

Valastyan S & Weinberg RA. (2011). Tumor Metastasis: Molecular Insights and Evolving Paradigms. *Cell* **147,** 275-292.

Valinsky WC, Touyz RM & Shrier A. (2018). Aldosterone, SGK1, and Ion Channels in the Kidney. *Clinical Science* **132,** 173-183.

Vang Mouritzen M & Jenssen H. (2018). Optimized Scratch Assay for in Vitro Testing of Cell Migration with an Automated Optical Camera. *Journal of Visualized Experiments***,** e57691.

Verrey F. (1995). Transcriptional Control of Sodium Transport in Tight Epithelia by Adrenal Steroids. *The Journal of Membrane Biology* **144,** 93-110.

Waldmann R, Champigny G, Bassilana F, Voilley N & Lazdunski M. (1995). Molecular Cloning and Functional Expression of a Novel Amiloride-Sensitive Na+ Channel. *Journal of Biological Chemistry* **270,** 27411-27414.

Wang Y & Zhou BP. (2011). Epithelial-Mesenchymal Transition in Breast Cancer Progression and Metastasis. *Chinese Journal of Cancer* **30,** 603-611.

Weigelt B, Geyer FC & Reis-Filho JS. (2010). Histological Types of Breast Cancer: How Special Are They? *Molecular Oncology* **4,** 192-208.

Yamamura H, Ugawa S, Ueda T & Shimada S. (2008). Expression Analysis of the Epithelial Na+ Channel δ Subunit in Human Melanoma G-361 Cells. *Biochemical and Biophysical Research Communications* **366,** 489-492.

Yang H-Y, Charles R-P, Hummler E, Baines DL & Isseroff RR. (2013). The Epithelial Sodium Channel Mediates the Directionality of Galvanotaxis in Human Keratinocytes. *Journal of Cell Science* **126,** 1942-1951.

Yang M, Ma B, Shao H, Clark AM & Wells A. (2016). Macrophage Phenotypic Subtypes Diametrically Regulate Epithelial-Mesenchymal Plasticity in Breast Cancer Cells. *BMC Cancer* **16,** 419-419.

Yu M, Bardia A, Wittner BS, Stott SL, Smas ME, Ting DT, Isakoff SJ, Ciciliano JC, Wells MN, Shah AM, Concannon KF, Donaldson MC, Sequist LV, Brachtel E, Sgroi D, Baselga J, Ramaswamy S, Toner M, Haber DA & Maheswaran S. (2013). Circulating Breast Tumor Cells Exhibit Dynamic Changes in Epithelial and Mesenchymal Composition. *Science* **339,** 580.

Zhang JT, Jiang XH, Xie C, Cheng H, Da Dong J, Wang Y, Fok KL, Zhang XH, Sun TT, Tsang LL, Chen H, Sun XJ, Chung YW, Cai ZM, Jiang WG & Chan HC. (2013). Downregulation of CFTR Promotes Epithelial-to-Mesenchymal Transition and Is Associated with Poor Prognosis of Breast Cancer. *Biochimica et Biophysica Acta - Molecular Cell Research* **1833,** 2961-2969.

Zhang Y & Weinberg RA. (2018). Epithelial-to-Mesenchymal Transition in Cancer: Complexity and Opportunities. *Frontiers of Medicine* **12,** 361-373.

Zhou J, Cheng Y, Tang L, Martinka M & Kalia S. (2017). Up-Regulation of SERPINA3 Correlates with High Mortality of Melanoma Patients and Increased Migration and Invasion of Cancer Cells. *Oncotarget* **8,** 18712-18725.

6 Appendices

6.1 RNA Extraction Protocol

RNA extraction protocol used in this project.

TGen BOCRU RNA Micro Prep Extraction w/Qiagen RNeasy Kit
Updated 5/21/2013 C. Mancini

Before Extraction:

1. Prepare fresh 80% EtOH in a 50 mL conical tube: Add 24 mL 100% EtOH to 6 mL Gibco Ultrapure Distilled H_2O.
2. Add four volumes of 100% EtOH to Buffer RPE.
3. Dissolve lyophilized Carrier RNA (poly-A) in 1 mL Gibco Ultrapure Distilled H_2O to make a concentrated solution of 310 ng/µL. Store at -20°C.
4. Dilute Carrier RNA to make a working solution of 4 ng/µL in Buffer RLT (Enough for 10 preps. Make a fresh dilution each time.):
   Add 5 µL concentrated Carrier RNA solution to 34µL RLT Buffer and pipet mix. Add 6 µL diluted Carrier RNA solution to 34µL RLT Buffer for a final concentration of 4 ng/uL.

RNA Extraction:

Bench steps are all at RT. Work quickly to maintain RNA integrity.

1. Samples are usually stored bulk and frozen at -80°C in Trizol.
2. Thaw for 5 min @ in a 65°C water bath. Loosen cells by flicking.
3. Aliquot 200 µL into a 500 µL microtube and refreeze remaining bulk sample.
4. Add 40 µL of chloroform.
5. Shake tube vigorously for 15 sec.
6. Incubate on bench for 5 min.
7. Centrifuge 10 min @ 16,000 x *g*.
8. Carefully pipet off aqueous phase top layer (~75 µL) and transfer into new 1.5 mL microtube. Avoid disrupting interphase even if some loss of the aqueous phase will be incurred.
9. Add one volume of 80% EtOH diluted with Gibco Ultrapure Distilled H_2O (~ 75 µL) and pipet mix. Do not centrifuge.
10. Add 5µL of diluted Carrier RNA (4ng/µL) to each sample.
11. Gently pipet mix.
12. Apply to Qiagen Micro-RNeasy Column (~155 µL) and close tube.
13. Centrifuge for 30 sec @ 9,300 x *g*.
14. Reapply the flow through to the column and close tube.
15. Centrifuge for 30 sec @ 9,300 x *g*.
16. Discard flow through but keep collection tube.
17. Add 700µL Buffer RW1 and close tube.
18. Centrifuge for 30 sec @ 9,300 x *g*.
19. Discard flow through and change collection tube.
20. Add 500µL Buffer RPE and close tube.
21. Centrifuge for 30 sec @ 9,300 x *g*.
22. Discard flow through but keep collection tube.
23. Add 500µL freshly prepared 80% EtOH and close tube.
24. Centrifuge for 2 min @ 9,300 x *g*.
25. Discard flow through and change collection tube.
26. Centrifuge for 5 minutes @ 16,000 x *g* with the tube lid open to dry column.
27. Transfer column to a new 1.5 mL microtube. Discard flow through and collection tube.
28. Add 10µL Gibco Ultrapure Distilled H_2O and close tube.
29. Centrifuge for 1 min @ 16,000 x *g* to elute.
30. Add a second 10µL Gibco Ultrapure Distilled H2O and close tube.
31. Centrifuge for 1 min @ 16,000 x *g* to elute.
32. Spec samples for concentration and run on Agilent 2100 Bioanalyzer using the Eukaryote RNA Nano program. Keep on ice and store at -80°C.

6.2 PCR Result Sheets

Within the Content Row:

- GAPDH = GAPDH Primers
- A/α-ENaC = α ENaC Primers
- D/δ-ENaC = δ ENaC Primers

Within the Sample Row:

- Date scratch assay cells were lysed
- MD = MDA-MB-231 Cells
- BT = BT-549 Cells
- OE = Overexpression Transfection with Plasmid DNA
- KD = Knockdown Transfection with siRNA
- C/C1/C2 = Control Experiments
- A/A1/A2 = α ENaC Experiments
- D/D1/D2 = δ ENaC Experiments
- WATER = Water Control
- -RT CTRL = Minus Reverse Transcriptase Enzyme Control

MD A&D OE (10-6-19) PCR PLATE

Content	A ENaC	A ENaC	A ENaC	D ENaC	D ENaC	D ENaC	GAPDH	GAPDH	GAPDH	GAPDH	GAPDH	GAPDH
Sample	MD-OE C1	MD-OE C1	MD-OE C1	MD-OE C1	MD-OE C1	MD-OE C1	MD-OE C1	MD-OE C1	MD-OE C1	-RT CTRL	-RT CTRL	-RT CTRL
Cq	24.49	24.36	24.26	26.03	25.89	26.01	16.00	15.85	15.95			
Content	A ENaC	A ENaC	A ENaC	D ENaC	D ENaC	D ENaC	GAPDH	GAPDH	GAPDH	GAPDH	GAPDH	GAPDH
Sample	MD-OE C2	MD-OE C2	MD-OE C2	MD-OE C2	MD-OE C2	MD-OE C2	MD-OE C2	MD-OE C2	MD-OE C2	-RT CTRL	-RT CTRL	-RT CTRL
Cq	24.22	24.08	24.34	25.57	25.46	25.69	15.83	15.75	15.78		37.07	40.46
Content	A ENaC	A ENaC	A ENaC	D ENaC	D ENaC	D ENaC	GAPDH	GAPDH	GAPDH	GAPDH	GAPDH	GAPDH
Sample	MD-OE A1	MD-OE A1	MD-OE A1	MD-OE A1	MD-OE A1	MD-OE A1	MD-OE A1	MD-OE A1	MD-OE A1	-RT CTRL	-RT CTRL	-RT CTRL
Cq	22.06	21.95	21.68	24.10	32.21	23.42	15.65	15.63	15.73	39.28	40.82	
Content	A ENaC	A ENaC	A ENaC	D ENaC	D ENaC	D ENaC	GAPDH	GAPDH	GAPDH	GAPDH	GAPDH	GAPDH
Sample	MD-OE A2	MD-OE A2	MD-OE A2	MD-OE A2	MD-OE A2	MD-OE A2	MD-OE A2	MD-OE A2	MD-OE A2	-RT CTRL	-RT CTRL	-RT CTRL
Cq	21.99	21.60	22.14	22.97	22.92	22.55	15.44	15.39	15.42	34.37	39.88	35.78
Content	A ENaC	A ENaC	A ENaC	D ENaC	D ENaC	D ENaC	GAPDH	GAPDH	GAPDH	GAPDH	GAPDH	GAPDH
Sample	MD-OE D1	MD-OE D1	MD-OE D1	MD-OE D1	MD-OE D1	MD-OE D1	MD-OE D1	MD-OE D1	MD-OE D1	-RT CTRL	-RT CTRL	-RT CTRL
Cq	24.10	23.90	23.65	23.44	23.85	22.59	15.54	15.50	15.53		39.63	35.61
Content	A ENaC	A ENaC	A ENaC	D ENaC	D ENaC	D ENaC	GAPDH	GAPDH	GAPDH	GAPDH	GAPDH	GAPDH
Sample	MD-OE D2	MD-OE D2	MD-OE D2	MD-OE D2	MD-OE D2	MD-OE D2	MD-OE D2	MD-OE D2	MD-OE D2	-RT CTRL	-RT CTRL	-RT CTRL
Cq	23.85	23.74	23.86	24.27	23.50	23.44	15.66	15.14	15.53	38.51	35.45	34.56
Content	A ENaC	A ENaC	A ENaC	D ENaC	D ENaC	D ENaC	GAPDH	GAPDH	GAPDH	GAPDH	GAPDH	GAPDH
Sample	WATER	WATER	WATER	WATER	WATER	WATER	WATER	WATER	WATER	-RT CTRL	-RT CTRL	-RT CTRL
Cq	33.91			32.12	32.46	31.17	29.52	40.14	39.30	35.46		40.48

MD A&D OE (3-8-19); MD-BT A&D OE (13-8-19); MD-BT KD (17-8-19) α-ENaC PCR PLATE

Content	GAPDH	GAPDH	GAPDH	α-ENaC	α-ENaC	α-ENaC	α-ENaC	α-ENaC	α-ENaC	GAPDH	GAPDH	GAPDH
Sample	MD-OE C1 (4/8)	MD-OE C1 (4/8)	MD-OE C1 (4/8)	MD-OE C1 (4/8)	MD-OE C1 (4/8)	MD-OE C1 (4/8)	MD-OE C2 (4/8)	MD-OE C2 (4/8)	MD-OE C2 (4/8)	MD-OE C2 (4/8)	MD-OE C2 (4/8)	MD-OE C2 (4/8)
Cq	15.77	15.69	15.33	25.65	25.84	26.01	25.46	25.18	25.39	15.08	15.13	15.42
Content	GAPDH	GAPDH	GAPDH	α-ENaC	α-ENaC	α-ENaC	α-ENaC	α-ENaC	α-ENaC	GAPDH	GAPDH	GAPDH
Sample	MD-OE A1 (4/8)	MD-OE A1 (4/8)	MD-OE A1 (4/8)	MD-OE A1 (4/8)	MD-OE A1 (4/8)	MD-OE A1 (4/8)	MD-OE A2 (4/8)	MD-OE A2 (4/8)	MD-OE A2 (4/8)	MD-OE A2 (4/8)	MD-OE A2 (4/8)	MD-OE A2 (4/8)
Cq	14.91	15.19	14.77	20.58	20.51	19.73	20.41	20.19	20.42	15.16	15.28	15.32
Content	GAPDH	GAPDH	GAPDH	α-ENaC	α-ENaC	α-ENaC	α-ENaC	α-ENaC	α-ENaC	GAPDH	GAPDH	GAPDH
Sample	MD-OE C (14/8)	MD-OE C (14/8)	MD-OE C (14/8)	MD-OE C (14/8)	MD-OE C (14/8)	MD-OE C (14/8)	BT-OE C (14/8)	BT-OE C (14/8)	BT-OE C (14/8)	BT-OE C (14/8)	BT-OE C (14/8)	BT-OE C (14/8)
Cq	15.59	15.49	15.14	25.03	24.49	26.34	29.80	29.77	30.21	14.80	14.90	16.38
Content	GAPDH	GAPDH	GAPDH	α-ENaC	α-ENaC	α-ENaC	α-ENaC	α-ENaC	α-ENaC	GAPDH	GAPDH	GAPDH
Sample	MD-OE A (14/8)	MD-OE A (14/8)	MD-OE A (14/8)	MD-OE A (14/8)	MD-OE A (14/8)	MD-OE A (14/8)	BT-OE A (14/8)	BT-OE A (14/8)	BT-OE A (14/8)	BT-OE A (14/8)	BT-OE A (14/8)	BT-OE A (14/8)
Cq	15.32	14.43	14.79	23.12	22.09	22.45	22.87	22.87	22.96	15.37	15.59	15.70
Content	GAPDH	GAPDH	GAPDH	α-ENaC	α-ENaC	α-ENaC	α-ENaC	α-ENaC	α-ENaC	GAPDH	GAPDH	GAPDH
Sample	MD-KD C (18/8)	MD-KD C (18/8)	MD-KD C (18/8)	MD-KD C (18/8)	MD-KD C (18/8)	MD-KD C (18/8)	BT-KD C (18/8)	BT-KD C (18/8)	BT-KD C (18/8)	BT-KD C (18/8)	BT-KD C (18/8)	BT-KD C (18/8)
Cq	13.47	14.37	12.58	24.96	25.23	24.77	30.57	30.40	30.77	14.24	14.50	14.88
Content	GAPDH	GAPDH	GAPDH	α-ENaC	α-ENaC	α-ENaC	α-ENaC	α-ENaC	α-ENaC	GAPDH	GAPDH	GAPDH
Sample	MD-KD A (18/8)	MD-KD A (18/8)	MD-KD A (18/8)	MD-KD A (18/8)	MD-KD A (18/8)	MD-KD A (18/8)	BT-KD A (18/8)	BT-KD A (18/8)	BT-KD A (18/8)	BT-KD A (18/8)	BT-KD A (18/8)	BT-KD A (18/8)
Cq	15.90	15.70	15.86	25.59	26.11	26.12	29.92	29.24	30.08	14.87	14.94	15.10
Content	GAPDH	GAPDH	GAPDH	α-ENaC	α-ENaC	α-ENaC	α-ENaC	α-ENaC	α-ENaC	GAPDH	GAPDH	GAPDH
Sample	WATER	WATER	WATER	WATER	WATER	WATER	WATER	WATER	WATER	WATER	WATER	WATER
Cq			36.07				35.35	33.83				

MD A&D OE (3-8-19); MD-BT A&D OE (13-8-19); MD-BT KD (17-8-19) δ-ENaC PCR PLATE

Content	GAPDH	GAPDH	GAPDH	δ-ENaC	δ-ENaC	δ-ENaC	δ-ENaC	δ-ENaC	δ-ENaC	GAPDH	GAPDH	GAPDH
Sample	MD-OE C1 (4/8)	MD-OE C1 (4/8)	MD-OE C1 (4/8)	MD-OE C1 (4/8)	MD-OE C1 (4/8)	MD-OE C1 (4/8)	MD-OE C2 (4/8)	MD-OE C2 (4/8)	MD-OE C2 (4/8)	MD-OE C2 (4/8)	MD-OE C2 (4/8)	MD-OE C2 (4/8)
Cq	15.95	15.20	15.25	25.84	25.91	26.00	25.01	25.02	25.14	14.57	14.85	15.07
Content	GAPDH	GAPDH	GAPDH	δ-ENaC	δ-ENaC	δ-ENaC	δ-ENaC	δ-ENaC	δ-ENaC	GAPDH	GAPDH	GAPDH
Sample	MD-OE D1 (4/8)	MD-OE D1 (4/8)	MD-OE D1 (4/8)	MD-OE D1 (4/8)	MD-OE D1 (4/8)	MD-OE D1 (4/8)	MD-OE D2 (4/8)	MD-OE D2 (4/8)	MD-OE D2 (4/8)	MD-OE D2 (4/8)	MD-OE D2 (4/8)	MD-OE D2 (4/8)
Cq	14.20	14.23	14.66	23.47	23.09	22.57	23.42	23.22	23.63	15.19	14.58	15.04
Content	GAPDH	GAPDH	GAPDH	δ-ENaC	δ-ENaC	δ-ENaC	δ-ENaC	δ-ENaC	δ-ENaC	GAPDH	GAPDH	GAPDH
Sample	MD-OE C (14/8)	MD-OE C (14/8)	MD-OE C (14/8)	MD-OE C (14/8)	MD-OE C (14/8)	MD-OE C (14/8)	BT-OE C (14/8)	BT-OE C (14/8)	BT-OE C (14/8)	BT-OE C (14/8)	BT-OE C (14/8)	BT-OE C (14/8)
Cq	15.63	15.16	15.19	25.74	25.39	26.02	25.93	25.74	25.96	15.21	15.34	15.75
Content	GAPDH	GAPDH	GAPDH	δ-ENaC	δ-ENaC	δ-ENaC	δ-ENaC	δ-ENaC	δ-ENaC	GAPDH	GAPDH	GAPDH
Sample	MD-OE D (14/8)	MD-OE D (14/8)	MD-OE D (14/8)	MD-OE D (14/8)	MD-OE D (14/8)	MD-OE D (14/8)	BT-OE D (14/8)	BT-OE D (14/8)	BT-OE D (14/8)	BT-OE D (14/8)	BT-OE D (14/8)	BT-OE D (14/8)
Cq	14.36	14.11	15.00	23.77	23.58	23.74	23.13	22.87	22.93	15.01	15.08	15.51
Content	GAPDH	GAPDH	GAPDH	δ-ENaC	δ-ENaC	δ-ENaC	δ-ENaC	δ-ENaC	δ-ENaC	GAPDH	GAPDH	GAPDH
Sample	MD-KD C (18/8)	MD-KD C (18/8)	MD-KD C (18/8)	MD-KD C (18/8)	MD-KD C (18/8)	MD-KD C (18/8)	BT-KD C (18/8)	BT-KD C (18/8)	BT-KD C (18/8)	BT-KD C (18/8)	BT-KD C (18/8)	BT-KD C (18/8)
Cq	14.18	14.08	14.07	25.16	25.29	25.22	25.84	25.90	26.07	14.15	14.28	14.46
Content	GAPDH	GAPDH	GAPDH	δ-ENaC	δ-ENaC	δ-ENaC	δ-ENaC	δ-ENaC	δ-ENaC	GAPDH	GAPDH	GAPDH
Sample	MD-KD D (18/8)	MD-KD D (18/8)	MD-KD D (18/8)	MD-KD D (18/8)	MD-KD D (18/8)	MD-KD D (18/8)	BT-KD D (18/8)	BT-KD D (18/8)	BT-KD D (18/8)	BT-KD D (18/8)	BT-KD D (18/8)	BT-KD D (18/8)
Cq	13.96	12.82	12.94	25.34	24.42	25.14	25.70	25.23	25.00	13.60	13.67	14.50
Content	GAPDH	GAPDH	GAPDH	δ-ENaC	δ-ENaC	δ-ENaC	δ-ENaC	δ-ENaC	δ-ENaC	GAPDH	GAPDH	GAPDH
Sample	WATER	WATER	WATER	WATER	WATER	WATER	WATER	WATER	WATER	WATER	WATER	WATER
Cq				31.86	32.23	32.19	32.12	31.88	32.08			

BT A&D OE (22-7-19); MD A&D OE (8-7-19); BT A&D OE (26-7-19) α-ENaC PCR PLATE

Content	GAPDH	GAPDH	GAPDH	α-ENaC	α-ENaC	α-ENaC	α-ENaC	α-ENaC	α-ENaC	GAPDH	GAPDH	GAPDH
Sample	BT C1 (23/7)	BT C1 (23/7)	BT C1 (23/7)	BT C1 (23/7)	BT C1 (23/7)	BT C1 (23/7)	BT C2 (23/7)	BT C2 (23/7)	BT C2 (23/7)	BT C2 (23/7)	BT C2 (23/7)	BT C2 (23/7)
Cq	16.49	16.80	16.07	33.41	31.12	32.10	33.87	36.18	31.17	17.14	16.55	17.38
Content	GAPDH	GAPDH	GAPDH	α-ENaC	α-ENaC	α-ENaC	α-ENaC	α-ENaC	α-ENaC	GAPDH	GAPDH	GAPDH
Sample	BT A1 (23/7)	BT A1 (23/7)	BT A1 (23/7)	BT A1 (23/7)	BT A1 (23/7)	BT A1 (23/7)	BT A2 (23/7)	BT A2 (23/7)	BT A2 (23/7)	BT A2 (23/7)	BT A2 (23/7)	BT A2 (23/7)
Cq	16.33	16.35	16.17	22.86	22.40	22.77	22.65	22.80	22.85	16.21	16.27	16.39
Content	GAPDH	GAPDH	GAPDH	α-ENaC	α-ENaC	α-ENaC	α-ENaC	α-ENaC	α-ENaC	GAPDH	GAPDH	GAPDH
Sample	MD C1 (9/7)	MD C1 (9/7)	MD C1 (9/7)	MD C1 (9/7)	MD C1 (9/7)	MD C1 (9/7)	MD C2 (9/7)	MD C2 (9/7)	MD C2 (9/7)	MD C2 (9/7)	MD C2 (9/7)	MD C2 (9/7)
Cq	16.24	16.19	16.18	25.70	25.57	25.59	24.30	24.47	24.85	16.17	15.45	15.81
Content	GAPDH	GAPDH	GAPDH	α-ENaC	α-ENaC	α-ENaC	α-ENaC	α-ENaC	α-ENaC	GAPDH	GAPDH	GAPDH
Sample	MD A1 (9/7)	MD A1 (9/7)	MD A1 (9/7)	MD A1 (9/7)	MD A1 (9/7)	MD A1 (9/7)	MD A2 (9/7)	MD A2 (9/7)	MD A2 (9/7)	MD A2 (9/7)	MD A2 (9/7)	MD A2 (9/7)
Cq	15.58	15.58	15.54	20.71	20.75	20.78	21.03	21.30	21.86	16.97	17.08	17.07
Content	GAPDH	GAPDH	GAPDH	α-ENaC	α-ENaC	α-ENaC	α-ENaC	α-ENaC	α-ENaC	GAPDH	GAPDH	GAPDH
Sample	BT C1 (27/7)	BT C1 (27/7)	BT C1 (27/7)	BT C1 (27/7)	BT C1 (27/7)	BT C1 (27/7)	BT C2 (27/7)	BT C2 (27/7)	BT C2 (27/7)	BT C2 (27/7)	BT C2 (27/7)	BT C2 (27/7)
Cq	14.85	15.53	15.55	31.91	31.44	30.49	31.19	30.48	32.26	15.92	15.28	15.93
Content	GAPDH	GAPDH	GAPDH	α-ENaC	α-ENaC	α-ENaC	α-ENaC	α-ENaC	α-ENaC	GAPDH	GAPDH	GAPDH
Sample	BT A1 (27/7)	BT A1 (27/7)	BT A1 (27/7)	BT A1 (27/7)	BT A1 (27/7)	BT A1 (27/7)	BT A2 (27/7)	BT A2 (27/7)	BT A2 (27/7)	BT A2 (27/7)	BT A2 (27/7)	BT A2 (27/7)
Cq	15.65	16.94	15.21	21.41	21.54	22.00	21.85	21.87	22.12	15.84	15.78	16.10
Content	GAPDH	GAPDH	GAPDH	α-ENaC	α-ENaC	α-ENaC	α-ENaC	α-ENaC	α-ENaC	GAPDH	GAPDH	GAPDH
Sample	WATER	WATER	WATER	WATER	WATER	WATER	WATER	WATER	WATER	WATER	WATER	WATER
Cq			39.30		35.82	34.53				35.00	38.84	35.89

BT A&D OE (22-7-19); MD A&D OE (8-7-19); BT A&D OE (26-7-19) δ-ENaC PCR PLATE

Content	GAPDH	GAPDH	GAPDH	δ-ENaC	δ-ENaC	δ-ENaC	δ-ENaC	δ-ENaC	δ-ENaC	GAPDH	GAPDH	GAPDH
Sample	BT C1 (23/7)	BT C1 (23/7)	BT C1 (23/7)	BT C1 (23/7)	BT C1 (23/7)	BT C1 (23/7)	BT C2 (23/7)	BT C2 (23/7)	BT C2 (23/7)	BT C2 (23/7)	BT C2 (23/7)	BT C2 (23/7)
Cq	17.23	17.06	16.34	26.08	25.50	24.77	24.49	25.71	26.28	16.48	14.34	15.55
Content	GAPDH	GAPDH	GAPDH	δ-ENaC	δ-ENaC	δ-ENaC	δ-ENaC	δ-ENaC	δ-ENaC	GAPDH	GAPDH	GAPDH
Sample	BT D1 (23/7)	BT D1 (23/7)	BT D1 (23/7)	BT D1 (23/7)	BT D1 (23/7)	BT D1 (23/7)	BT D2 (23/7)	BT D2 (23/7)	BT D2 (23/7)	BT D2 (23/7)	BT D2 (23/7)	BT D2 (23/7)
Cq	16.42	15.34	15.13	21.61	20.75	22.39	22.36	22.33	22.11	15.71	15.90	16.40
Content	GAPDH	GAPDH	GAPDH	δ-ENaC	δ-ENaC	δ-ENaC	δ-ENaC	δ-ENaC	δ-ENaC	GAPDH	GAPDH	GAPDH
Sample	MD C1 (9/7)	MD C1 (9/7)	MD C1 (9/7)	MD C1 (9/7)	MD C1 (9/7)	MD C1 (9/7)	MD C2 (9/7)	MD C2 (9/7)	MD C2 (9/7)	MD C2 (9/7)	MD C2 (9/7)	MD C2 (9/7)
Cq	16.35	15.93	15.65	25.77	25.68	25.95	26.39	26.39	26.20	15.92	16.20	16.30
Content	GAPDH	GAPDH	GAPDH	δ-ENaC	δ-ENaC	δ-ENaC	δ-ENaC	δ-ENaC	δ-ENaC	GAPDH	GAPDH	GAPDH
Sample	MD D1 (9/7)	MD D1 (9/7)	MD D1 (9/7)	MD D1 (9/7)	MD D1 (9/7)	MD D1 (9/7)	MD D1 (9/7)	MD D1 (9/7)	MD D1 (9/7)	MD D1 (9/7)	MD D1 (9/7)	MD D1 (9/7)
Cq	15.49	15.24	15.17	22.01	21.96	22.02	23.07	22.94	23.22	15.47	15.56	15.96
Content	GAPDH	GAPDH	GAPDH	δ-ENaC	δ-ENaC	δ-ENaC	δ-ENaC	δ-ENaC	δ-ENaC	GAPDH	GAPDH	GAPDH
Sample	BT C1 (27/7)	BT C1 (27/7)	BT C1 (27/7)	BT C1 (27/7)	BT C1 (27/7)	BT C1 (27/7)	BT C2 (27/7)	BT C2 (27/7)	BT C2 (27/7)	BT C2 (27/7)	BT C2 (27/7)	BT C2 (27/7)
Cq	15.37	15.79	15.44	25.76	25.79	24.87	26.20	25.38	26.02	15.94	16.05	16.30
Content	GAPDH	GAPDH	GAPDH	δ-ENaC	δ-ENaC	δ-ENaC	δ-ENaC	δ-ENaC	δ-ENaC	GAPDH	GAPDH	GAPDH
Sample	BT D1 (27/7)	BT D1 (27/7)	BT D1 (27/7)	BT D1 (27/7)	BT D1 (27/7)	BT D1 (27/7)	BT D2 (27/7)	BT D2 (27/7)	BT D2 (27/7)	BT D2 (27/7)	BT D2 (27/7)	BT D2 (27/7)
Cq	15.54	16.10	15.56	21.72	22.85	22.04	23.24	23.22	22.06	15.31	14.78	16.33
Content	GAPDH	GAPDH	GAPDH	δ-ENaC	δ-ENaC	δ-ENaC	δ-ENaC	δ-ENaC	δ-ENaC	GAPDH	GAPDH	GAPDH
Sample	WATER	WATER	WATER	WATER	WATER	WATER	WATER	WATER	WATER	WATER	WATER	WATER
Cq	38.30	38.79	35.19	32.69	31.51	32.67	32.17	31.90	31.95	37.27	38.51	37.78

MD-BT A&D KD (14-8-19); MD A&D KD (26-8-19) PCR PLATE

Content	GAPDH	GAPDH	GAPDH	α-ENaC	α-ENaC	α-ENaC	δ-ENaC	δ-ENaC	δ-ENaC			
Sample	C MD-KD 15/8	C MD-KD 15/8	C MD-KD 15/8	C MD-KD 15/8	C MD-KD 15/8	C MD-KD 15/8	C MD-KD 15/8	C MD-KD 15/8	C MD-KD 15/8			
Cq	19.21	17.93	17.64	25.60	25.86	26.06	27.23	27.15	27.25			
Content	GAPDH	GAPDH	GAPDH	α-ENaC	α-ENaC	α-ENaC	δ-ENaC	δ-ENaC	δ-ENaC	GAPDH	GAPDH	GAPDH
Sample	A MD-KD 15/8	A MD-KD 15/8	A MD-KD 15/8	A MD-KD 15/8	A MD-KD 15/8	A MD-KD 15/8	D MD-KD 15/8	D MD-KD 15/8	D MD-KD 15/8	D MD-KD 15/8	D MD-KD 15/8	D MD-KD 15/8
Cq	18.28	17.74	17.71	25.89	25.94	25.76	27.02	26.81	26.65		17.76	17.97
Content	GAPDH	GAPDH	GAPDH	α-ENaC	α-ENaC	α-ENaC	δ-ENaC	δ-ENaC	δ-ENaC			
Sample	C BT-KD 15/8	C BT-KD 15/8	C BT-KD 15/8	C BT-KD 15/8	C BT-KD 15/8	C BT-KD 15/8	C BT-KD 15/8	C BT-KD 15/8	C BT-KD 15/8			
Cq	17.65	17.85	17.46	32.20	32.70	32.52	27.97	27.76	27.88			
Content	GAPDH	GAPDH	GAPDH	α-ENaC	α-ENaC	α-ENaC	δ-ENaC	δ-ENaC	δ-ENaC	GAPDH	GAPDH	GAPDH
Sample	A BT-KD 15/8	A BT-KD 15/8	A BT-KD 15/8	A BT-KD 15/8	A BT-KD 15/8	A BT-KD 15/8	D BT-KD 15/8	D BT-KD 15/8	D BT-KD 15/8	D BT-KD 15/8	D BT-KD 15/8	D BT-KD 15/8
Cq	18.38	18.16	18.20	34.45	33.18	32.76	28.03	27.62	28.12	17.93	17.99	18.22
Content	GAPDH	GAPDH	GAPDH	α-ENaC	α-ENaC	α-ENaC	δ-ENaC	δ-ENaC	δ-ENaC			
Sample	C MD-KD 27/8	C MD-KD 27/8	C MD-KD 27/8	C MD-KD 27/8	C MD-KD 27/8	C MD-KD 27/8	C MD-KD 27/8	C MD-KD 27/8	C MD-KD 27/8			
Cq	17.68	17.47	17.37	24.82	24.89	24.73	26.10	25.99	26.11			
Content	GAPDH	GAPDH	GAPDH	α-ENaC	α-ENaC	α-ENaC	δ-ENaC	δ-ENaC	δ-ENaC	GAPDH	GAPDH	GAPDH
Sample	A MD-KD 27/8	A MD-KD 27/8	A MD-KD 27/8	A MD-KD 27/8	A MD-KD 27/8	A MD-KD 27/8	D MD-KD 27/8	D MD-KD 27/8	D MD-KD 27/8	D MD-KD 27/8	D MD-KD 27/8	D MD-KD 27/8
Cq	18.17	17.69	17.80	24.52	24.75	24.57	26.75	26.63	26.78		18.06	18.31
Content	GAPDH	GAPDH	GAPDH	α-ENaC	α-ENaC	α-ENaC	δ-ENaC	δ-ENaC	δ-ENaC			
Sample	WATER	WATER	WATER	WATER	WATER	WATER	WATER	WATER	WATER			
Cq							31.96	31.96	31.67			

MD A&D OE (17-6-19) PCR PLATE

Content	A ENaC	A ENaC	A ENaC	D ENaC	D ENaC	D ENaC	GAPDH	GAPDH	GAPDH
Sample	MD-OE C1	MD-OE C1	MD-OE C1	MD-OE C1	MD-OE C1	MD-OE C1	MD-OE C1	MD-OE C1	MD-OE C1
Cq	25.22	24.43	24.48	25.69	25.62	25.63	16.30	16.34	16.43
Content	A ENaC	A ENaC	A ENaC	D ENaC	D ENaC	D ENaC	GAPDH	GAPDH	GAPDH
Sample	MD-OE C2	MD-OE C2	MD-OE C2	MD-OE C2	MD-OE C2	MD-OE C2	MD-OE C2	MD-OE C2	MD-OE C2
Cq	24.96	24.62	24.62	26.02	26.09	25.95	16.18	16.09	16.34
Content	A ENaC	A ENaC	A ENaC				GAPDH	GAPDH	GAPDH
Sample	MD-OE A1	MD-OE A1	MD-OE A1				MD-OE A1	MD-OE A1	MD-OE A1
Cq	22.89	22.54	22.59				16.30	16.23	16.30
Content	A ENaC	A ENaC	A ENaC				GAPDH	GAPDH	GAPDH
Sample	MD-OE A2	MD-OE A2	MD-OE A2				MD-OE A2	MD-OE A2	MD-OE A2
Cq	22.10	21.71	21.98				15.96	15.74	16.07
Content				D ENaC	D ENaC	D ENaC	GAPDH	GAPDH	GAPDH
Sample				MD-OE D1	MD-OE D1	MD-OE D1	MD-OE D1	MD-OE D1	MD-OE D1
Cq				25.30	25.45	25.26	15.90	16.16	16.00
Content				D ENaC	D ENaC	D ENaC	GAPDH	GAPDH	GAPDH
Sample				MD-OE D2	MD-OE D2	MD-OE D2	MD-OE D2	MD-OE D2	MD-OE D2
Cq				23.03	23.03	23.17	16.11	15.90	16.09
Content	A ENaC	A ENaC	A ENaC	D ENaC	D ENaC	D ENaC	GAPDH	GAPDH	GAPDH
Sample	Water	Water	Water	Water	Water	Water	Water	Water	Water
Cq	38.16	34.15		33.98	33.21	32.43		38.27	40.61